ECOLE POLYTECNIQUE DE LOUVAIN – DEPARTAMENT D'ELECTRICITÉ

UNIVERSITÉ CATHOLIQUE DE LOUVAIN

Final Career Project

Channel Modelling for Distributed Indoor Wireless Networks

Authors: Mariem Herrero Medina

Cristian Sánchez-Camacho Yebra

Director: Claude Oestges

Co-Director: Olivier Renaudin

Authors	Mariem Herrero Medina Cristian Sánchez-Camacho Yebra
Emails authors	mariem.herreromedina@gmail.com cristian.yebra @gmail.com
Director	Claude Oestges
Email director	claude.oestges@uclouvain.be
Co-director	Olivier Renaudin
Email co-director	olivier.renaudin@uclouvain.be
Title of FCP	Channel Modelling for Distributed Indoor Channel Networks
Key words	WLAN, SISO, MIMO, indoor, characterization, modelling, path loss, static shadowing, dynamic shadowing, correlation, fading, wireless, Kronecker

Abstract

Since the launch of the wireless local area networks (WLAN) based on the 802.11b, 802.11g and 802.11n standards, a growing interest to this technology has appeared. Actually practically all the colleges, universities, hospitals and public buildings have a WLAN. For this reason is a field constantly studied and improved.

This work is an experimental characterisation and modelling of indoor-to-indoor distributed channels using SISO (Single-Input Single-Output) and MIMO (Multiple-Input Multiple-Output) systems and experimental data in the 3.8 GHz band.

The difference between SISO and MIMO systems lies on the number of transmitting and receiving antennas. The first system consists in one transmitter and one receiver and the second in N transmitters and M receivers. The discovery of the MIMO systems was caused by the request of a higher speed transmission and more quality system than the one SISO offered. Through the space-time codification or flux multiplexing it is possible to obtain spatial diversity in transmission which increases the quality of the link or create different parallel channels which increase the global spectral efficiency.

The scenario is the first floor of a building of the UCL (Université Catholique de Louvain) and is an office environment. The measurements, hence the data collection, were taken in a campaign made in October 2009. The experimental set-up is defined in the paper 'PUCCO Radio Measurement Campaign'.

We have different scenarios and topologies and the parameters studied in SISO are basically, path loss, shadowing and fading. We distinguish between different types of indoor node mobility with respect the transmitter and/or receiver nodes. These types are three: single-mobile, double-mobile and static or nomadic nodes. In MIMO one of the most important factors is the correlation, which value shows the independence level among the subchannels generated among transmitter antennas and receiver antennas. We try to find if the MIMO channels measured can be modelled by the Kronecker model.

Our work has been to analyze the data achieved in the experiment by creating different scripts with Matlab.

Graduate	Ingenieria Técnica de Telecomunicaciones especialidad Telemática
Department	Ecole Polytecnique de Louvain - Departament d'Electricité
Date of presentation	June 11th 2010

ABSTRACT

Since the launch of the wireless local area networks (WLAN) based on the 802.11b, 802.11g and 802.11n standards, a growing interest to this technology has appeared. Actually practically all the colleges, universities, hospitals and public buildings have a WLAN. For this reason is a field constantly studied and improved.

This work is an experimental characterisation and modelling of indoor-to-indoor distributed channels using SISO (Single-Input Single-Output) and MIMO (Multiple-Input Multiple-Output) systems and experimental data in the 3.8 GHz band.

The difference between SISO and MIMO systems lies on the number of transmitting and receiving antennas. The first system consists in one transmitter and one receiver and the second in N transmitters and M receivers. The discovery of the MIMO systems was caused by the request of a higher speed transmission and more quality system than the one SISO offered. Through the space-time codification or flux multiplexing it is possible to obtain spatial diversity in transmission which increases the quality of the link or create different parallel channels which increase the global spectral efficiency.

The scenario is the first floor of a building of the UCL (Université Catholique de Louvain) and is an office environment. The measurements, hence the data collection, were taken in a campaign made in October 2009. The experimental set-up is defined in the paper 'PUCCO Radio Measurement Campaign'.

We have different scenarios and topologies and the parameters studied in SISO are basically, path loss, shadowing and fading. We distinguish between different types of indoor node mobility with respect the transmitter and/or receiver nodes. These types are three: single-mobile, double-mobile and static or nomadic nodes. In MIMO one of the most important factors is the correlation, which value shows the independence level among the subchannels generated among transmitter antennas and receiver antennas. We try to find if the MIMO channels measured can be modelled by the Kronecker model.

Our work has been to analyze the data achieved in the experiment by creating different scripts with Matlab.

INDEX

List of Figures 9

List of Tables 11

PART 0. Experimental Characterization of the Radio Channel

1. Introduction 14

2. Indoor-to-Indoor (I2I) Measurements 14

2.1. Measurements setup and practice 14

2.2. Sounding parameters 15

2.3. Scenarios 16

2.3.1. Distributed antennas: 16 nodes (SISO) 16

2.3.2. Distributed antennas: 8 nodes (MIMO) 17

2.4. Equipment 18

2.4.1. Elektrobit Propsound Channel Sounder 18

2.4.2. Antennas 19

2.4.3. RF cables 19

PART 1. Single Antenna Analysis

Chapter 1. Introduction 21

Chapter 2. General Concepts 23

2.1. Path Loss 23

2.2. Shadowing 24

2.2.1. Static Shadowing 24

2.2.2. Dynamic Shadowing 25

2.3. Fading 26

Chapter 3. Process 28
3.1. Path Loss 29
3.2. Static Shadowing 30
3.3. Dynamic Shadowing 31
3.4. Fading 33
Chapter 4. Results 34
4.1. Path Loss and Static Shadowing 34
4.1.1. Tables 34
4.1.1.1. Static links 34
4.1.1.2. Dynamic links 39
4.1.2. Graphs 41
4.1.2.1. Scenario 16s 41
4.1.2.2. Scenario 16sp 41
4.1.2.3. Scenario 16ms 42
4.1.2.4. Scenario 16mLs 43
4.1.2.5. Scenario 16rms 44
4.1.2.6. All scenarios 45
4.2. Dynamic Shadowing 47
4.2.1. Autocorrelation 49
4.2.2. Cross-correlation 50
4.2.3. Standard deviation 51
4.3. Fading 52
4.3.1. Static nodes 52
4.3.2. Mobile nodes 54
4.4. Model parameters 57
Chapter 5. Conclusions 58

PART 2. Multiple Antenna Analysis

Chapter 1. Introduction 61

Chapter 2. General Concepts 62

2.1. Introduction 62

2.2. Antenna Configurations 63

2.3. Channel Matrix 63

2.4. Basis of MIMO systems 64

2.4.1. Spatial multiplexing gain 64

2.4.2. Diversity gain 64

2.4.3. Array gain 64

2.5. Spatial Diversity 65

2.5.1. Spatial Diversity in Reception 65

2.5.2. Spatial Diversity in Transmission 65

2.5.2.1. Space-time Coding 65

2.5.2.2. Spatial Multiplexing 66

2.6. Spatial correlation 66

2.7. Capacity 67

2.8. Analytical Channel Models 67

2.8.1. Simplified Representation of Gaussian MIMO Channels 67

2.8.1.1. Kronecker model 68

2.8.1.2. Eigenbeam model from Weichselberger model 68

2.8.1.3. Virtual Channel Representation 69

Chapter 3. Process 70

3.1. Obtaining the Channel Matrix 70

3.2. Obtaining the Spatial Correlation Matrix 71

3.3. Obtaining the Kronecker Model Correlation Matrix 72

3.4. Comparing Models and Correlations Matrices 72

Chapter 4. Results 73

4.1. Evolution of Ψ and d_{corr} in time 73

4.2. Relation between d_{corr} and α 76

4.3. Relation between d_{corr} and Distance among nodes 77

Chapter 5. Conclusions 78

BIBLIOGRAPHY 79

List of figures

0.2.1. Map of the Scenario 15
0.2.2. Map of SISO configuration 17
0.2.3. Map of MIMO configuration 18
0.2.4. Picture of node antenna 19
0.2.5. Radiation pattern of the node antenna 19

1.2.1. Signal over time 26
1.4.1. Alpha-beta relation for static links 36
1.4.2. Fitting error histogram 37
1.4.3. Alpha-beta relation vs distance 37
1.4.4. Obstruction shadowing 38
1.4.5. Distribution of obstruction shadowing 38
1.4.6. Path loss fitting – scenario 16s (static links) 41
1.4.7. Path loss fitting – scenario 16sp (static links) 41
1.4.8. Path loss fitting – scenario 16ms (static links) 42
1.4.10. Path loss fitting – scenario 16ms (mobile links) 42
1.4.11. Path loss fitting – scenario 16mls (static links) 43
1.4.12. Path loss fitting – scenario 16mls (mobile links) 43
1.4.13. Path loss fitting – scenario 16rms (static links) 44
1.4.14. Path loss fitting – scenario 16rms (mobile links) 44
1.4.15. Path loss fitting – all scenarios (static links) 45
1.4.16. Path loss fitting – all scenarios (mobile links) 45
1.4.17. Contribution eta parameter (static links) 46
1.4.18. Contribution eta parameter (mobile links) 46
1.4.19. Dynamic shadowing signal of all subbands 47
1.4.20. Distribution of dynamic shadowing 47
1.4.21. Dynamic shadowing of static link 48
1.4.22. Dynamic shadowing of single-mobile link 48
1.4.23. Dynamic shadowing of double-mobile link 48

1.4.24. Dynamic shadowing temporal autocorrelation fitting 49
1.4.25. Std dynamic shadowing vs path loss 51
1.4.26. Std dynamic shadowing distribution 52
1.4.27. Fading behaviour in static links 52
1.4.28. Links where fading is practically constant along the time 53
1.4.29. Links where fading varies along the time 53
1.4.30. K-factor vs distance 54
1.4.31. Fading behaviour in single-mobile links 54
1.4.32. Fading behaviour in double-mobile links 55
1.4.33. Single-mobile links where fading is practically constant along the time 55
1.4.34. Double-mobile links where fading is practically constant along the time 56
1.4.35. Single-mobile links where fading varies along the time 56
1.4.36. Double-mobile links where fading varies along the time 57

2.2.1. Scheme of antenna configurations in a MIMO system 63
2.2.2. Scheme of subchannels generated in a MIMO system 64
2.2.3. Signal combining 65
2.4.1. Evolution of Ψ and dcorr in time - static links 73
2.4.2. Evolution of Ψ and dcorr in time – single-mobile links 74
2.4.3. Evolution of Ψ and dcorr in time – double-mobile links 74
2.4.5. D_{corr} vs α for single-mobile links 76
2.4.6. D_{corr} vs α for double-mobile links 76
2.4.7. D_{corr} vs distance for static links 77
2.4.8. D_{corr} vs distance for single-mobile links 77
2.4.9. D_{corr} vs distance for double-mobile links 77

List of tables

0.2.1. Sounding parameters 16
0.2.2. Configuration of deployed antennas 16
0.2.3. Distance among SISO nodes 17
0.2.4. Distance among MIMO nodes 18

1.4.1. Path loss and static shadowing model 1 (static links) 34
1.4.2. Path loss and static shadowing model 2 (static links) 35
1.4.3. Path loss and static shadowing model 3 (static links) 35
1.4.4. Path loss and static shadowing model 4 (static links) 35
1.4.5. Path loss and static shadowing model 1 (mobile links) 39
1.4.6. Path loss and static shadowing model 2 (mobile links) 39
1.4.7. Path loss and static shadowing model 3 (mobile links) 39
1.4.8. Path loss and static shadowing model 4 (mobile links) 39
1.4.9. Slope of dynamic shadowing temporal autocorrelation (20 samples) 49
1.4.10. Slope of dynamic shadowing temporal autocorrelation (10 samples) 49
1.4.11. Dynamic shadowing cross-correlation coefficients (20 samples) 50
1.4.12. Dynamic shadowing cross-correlation coefficients (10 samples) 50
1.4.18. SISO model parameters 57

2.4.1. Ψ (R, R') for 2x2 system 75
2.4.2. D_{corr} (R, R') for 2x2 system 75

PART 0.

Experimental Characterization of the Radio Channel

1. Introduction

The design of a communication system requires knowing accurately the propagation of the signal through the radio channel. This propagation is different for each scenario, due to the environment, position of the antennas, obstacles (walls, furniture...), distance among antennas...

The measurement campaign [1] is intended to encompass two distinct scenarios:

- ***Indoor-to-Indoor (I2I)*** measurements with nodes (single or grouped antennas) located in different parts of the building.
- ***Outdoor-to-Indoor (O2I)*** measurements where a base station (BS) will broadcast into an office building where there are a series of users present, each being equipped with one or more antennas.

Also there are different mobility scenarios:

- The antennas and the environment are static (e.g. no moving people).
- The antennas are static but the environment is not static (e.g. moving people).
- The antennas moving locally over small scales (e.g. 1 meter of radius).
- The antennas moving over larges scales (e.g. along a route in a corridor).

The antennas or nodes could be considered as users' stations.

In our study, we only treat with Indoor-to-Indoor (I2I) scenario and all types of mobility scenarios.

2. Indoor-to-Indoor (I2I) Measurements

These measurements are taken in an office environment at the first floor of a building, called Stevin, of the UCL (Université Catholique de Louvain). The objective is to consider transmitter (Tx) and receiver (Rx) nodes in the different mobility scenarios. A map of the indoor office environment is given in the Figure 0.2.1.

2.1. Measurement setup and practice

DP200908 omnidirectional dipole antennas were used throughout the I2I campaign (see Section 2.4.2.). These antennas are connected to the channel sounder switching units by means of various 32 m RF cables which are described in Section 2.4.3. There are 8 connections at either sounder unit allowing for experimental investigation of up to 16 nodes. Practically, antennas 1 to 8 were always connected by cables 1 to 8 to ports 1 to 8 of the Rx

unit. Similarly, antennas 9 to 16 were connected by cables 9 to 16 to ports 1 to 8 of the Tx unit. When using antenna arrays, these antennas were screwed along a line on a wooden support, with an antenna spacing of 3.95 cm (half-wavelength).

The indoor positions were first marked by duct tape on the floor. Fixed antennas were attached to desks by means of duct tape or carried out by people. Mobile antennas were always carried out by people. When considering fixed antennas, two kind of scenarios were measured: a fully static case (in the absence of moving people in corridors), and a dynamic case, when people moved along the corridor. To gather more data and check for artefacts, each measurement route was carried out twice. Note that some measurements might show a certain level of bursty interference. This interference must be eliminated in the post processing.

Finally, since the nature of these measurements is such that the Rx sounder unit and the Tx sounder unit were co-located, the channel sounder was used in single clock mode which means that both the Tx and Rx units shared a common clock signal.

FIGURE 0.2.1. MAP OF THE SCENARIO

2.2. Sounding parameters

The exact sounding parameters are provided in Table 0.2.1. A burst mode was used, meaning that each 8×8 MIMO channel (i.e. each cycle) was measured by bursts to increase the SNR, with a high cycle rate within a burst.

Parameter	Value
Carrier frequency [GHz]	3.8
Transmit power [dBm]	23
Bandwith [MHz]	50
No. Tx antennas	8
No. Rx antennas	8
Effective burst rate [Hz]	2.65
Burst length (No. Cycles/burst)	4
Channel rate (within a burst) [Hz]	21.203
Code length (No. chips)	2047 (distributed) – 4095 (clustered)
No. Samples/chip	2
Measurement length (No. Measured cycles)	1200

TABLE 0.2.1. SOUNDING PARAMETERS

Given the above values, it is straightforward to calculate that the duration of one measurement run was

$$\frac{\left(\frac{1200}{4}\right)}{2.65} = 113.2\ s$$

2.3. Scenarios

Given a total of 16 nodes may be supported, Table 0.2.2. shows the different SISO/MIMO configurations deployed.

No. of Nodes	No. of antennas at each node	Type
16	1	SISO
8	2	MIMO

TABLE 0.2.2. CONFIGURATION OF DEPLOYED ANTENNAS

All the nodes are located in different office rooms.

2.3.1. Distributed antennas: 16 nodes (SISO)

For 16 nodes (users), we consider the five following scenarios:

- ***16s*:** all 16 nodes are static, with no people in the area.
- ***16sp*:** all 16 nodes are static, with people passing by.
- ***16ms*:** 8 nodes are moving locally over a small range and 8 nodes are static.
- ***16mLs*:** 8 nodes are moving over a large range and 8 nodes are static.
- ***16rms:*** 2 nodes are moving along routes in the corridor, 6 nodes are moving locally over a small range and 8 nodes are static.

The Figure 0.2.2. is a scheme of this configuration.

FIGURE 0.2.2. MAP OF SISO CONFIGURATION

In the Table 0.2.3. there is the distance in meters among transmitter and receiver nodes.

	1	2	3	4	5	6	7	8	Rx
9	5,236	5,423	12,716	19,261	24,31	17,765	11,594	7,106	
10	12,529	3,179	4,675	11,781	18,887	14,212	11,22	12,155	
11	18,887	10,098	3,366	5,423	11,594	8,228	9,537	14,212	
12	28,05	19,261	11,594	4,862	5,049	8,976	15,334	21,879	
13	26,18	18,513	12,716	8,789	3,74	3,553	10,846	17,952	
14	20,757	14,586	11,407	11,22	10,098	2,805	4,488	11,594	
15	12,342	8,228	10,659	15,147	18,139	11,033	4,301	4,301	
16	8,228	13,277	19,635	25,245	28,237	20,944	13,651	6,545	
Tx									

TABLE 0.2.3. DISTANCE AMONG SISO NODES

2.3.2. Distributed antennas: 8 nodes (MIMO)

For 8 nodes, we consider the five following scenarios:

- ***8s:*** all 8 nodes are static, with no people in the area.
- ***8sp:*** all 8 nodes are static, with people passing by.
- ***8ms:*** 4 nodes are moving locally over a small range and 4 nodes are static.

- ***8rms:*** 2 nodes are moving along routes in the corridor, 2 nodes are moving locally over a small range and 4 nodes are static.

In the Figure 0.2.3. we present a scheme of this configuration.

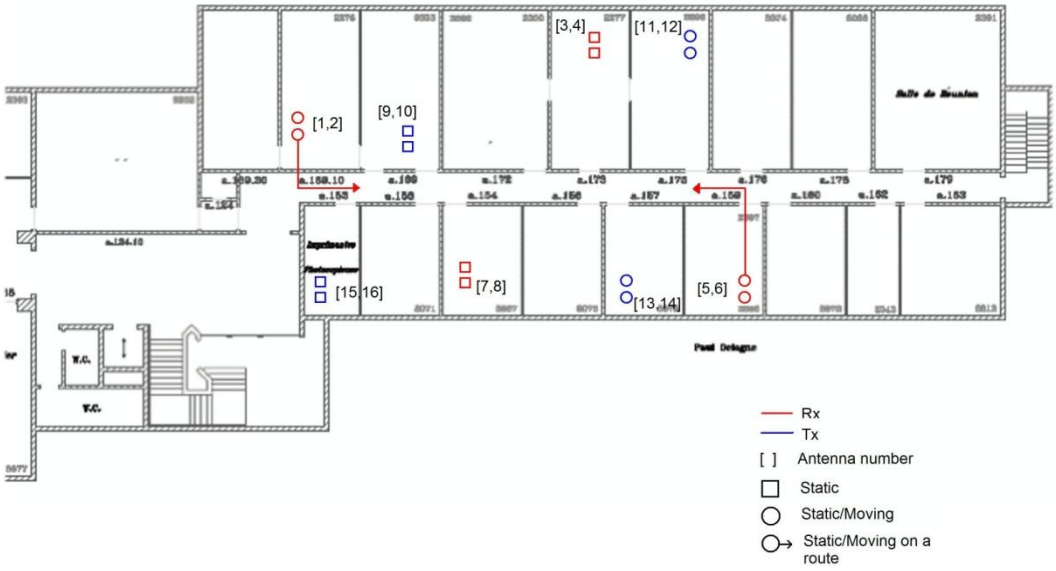

FIGURE 0.2.3. MAP OF MIMO CONFIGURATION

The table 0.2.4. shows the distance in meters among nodes.

	[1,2]	[3,4]	[5,6]	[7,8]	Rx
[9,10]	4,488	9,163	15,895	6,919	
[11,12]	17,017	4,0205	11,22	14,025	
[13,14]	16,5495	11,22	4,2075	7,1995	
[15,16]	7,48	14,96	18,0455	6,545	
Tx					

TABLE 0.2.4. DISTANCE AMONG MIMO NODES

2.4. Equipment

2.4.1. Elektrobit Propsound Channel Sounder

The Elektrobit propsound channel sounder is capable of measuring up to 8×8 MIMO channels at a center frequency of 3.8 GHz. The bandwidth is scalable up to 200 MHz maximum around the central frequency. The sounder utilizes the switched-array principle, i.e. only one link between a specific Rx element and Tx element is measured at a time (using

only one transmitter and one receiver chain), while switches at the Tx and Rx sounding units select the link to be measured. The time for measuring one complete MIMO matrix thus depends on the number of Tx and Rx antennas used, and on the length of the cannel sounding sequence. A pre-measurement campaign will further define the sounder set-up.

2.4.2. Antennas

The node antennas are highly efficient dipole antennas with an almost isotropic radiation pattern, which is reflected by the fact that their antenna gain is only 1.75 dBi. They utilise an optimised quarter wave current trap principle and are protected from shock by a Rohacell jacketing. They are equipped with SMA female connectors and have an input impedance of 50. They can operate efficiently within a bandwidth of 3.7 GHz to 3.9 GHz and have maximum radiation efficiency at 3.8 GHz. They are clearly numbered from 1 to 16, and can be easily screwed on a wooden support (for building antenna arrays).

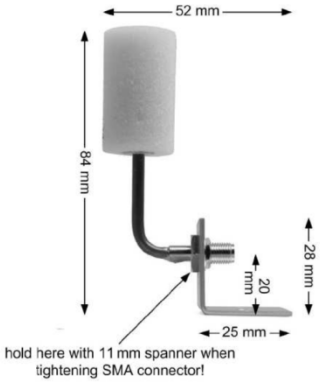

FIGURE 0.2.4. PICTURE OF NODE ANTENNA

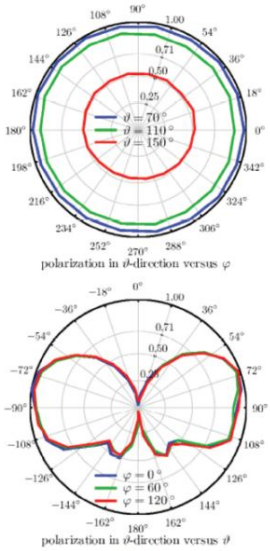

FIGURE 0.2.5. RADIATION PATTERN OF THE NODE ANTENNA

2.4.3. RF cables

For the I2I campaign, 32 m cables are being used by all of the nodes (from each node to the switching unit). These cables were measured and their average loss was 8.76 dB at 3.8 GHz (±0.01 dB).

PART 1.

Single Antenna Analysis (SISO)

Chapter 1.

Introduction

The human necessity of being communicated around the world launches the idea of radio communications which are based in the transmission between antennas. The easiest and classic way of radio communication is the one called SISO, Single-Input Single-Output. SISO refers to the antenna technology that uses one transmitting and one receiving antenna.

Many of the expectations of the wireless technologies in the last years had not been accomplished. Technologies like Bluetooth or that linked with the third generation (3G) are practically simples promises and they are not much implanted. In the computing field, the wireless technologies (WLANs Wireless Local Area Network) had been quickly extended. Actually, the nets WLAN are installed in universities, offices, hospitals, homes and even in public spaces. For this reason is a field constantly studied and improved.

Normally, the WLANs are computers or portables connected via radio signals to fixed devices called 'access points'. Through the development of standards, different wireless devices can be mixed making and access more direct and transparent with the technology. The standards are developed by international recognized organisms, like the IEEE (Institute of Electrical and Electronics Engineers) and the ETSI (European Telecommunications Standards Institute). Once developed, they become the basis of manufacturers to develop their products.

Great progresses have been realized in modulation, codification and signal processing to maximize the spectral efficiency with the purpose of covering the high speed transmission and quality in communications request. But this has not been enough, in digital communication systems this technology is vulnerable to the environment and fading causing the reduction in data speed and an increase in the number of errors.

The SISO technology can be used to implement a cooperative communication, a promising technology which goal is to increase coverage, reliability and spectral efficiency [2]. Cooperative communication refers to processing of this overheard information at the surrounding nodes and retransmission towards the destination to create spatial diversity, thereby to obtain higher throughput and reliability [4].

This Part1 is dedicated to study the measurements made in a building floor which specifications are explained in Part0 where the channels are among eight transmitters and eight receivers.

The content of this part is structured in five chapters. On Chapter 2 are introduced the general concepts of the data analysis covering the parameters and magnitudes that compose a channel: Path Loss, Shadowing (which includes in turn Static and Dynamic Shadowing) and Fading. On Chapter 3 is described the process to obtain the parameters above mentioned. On Chapter 4 are exposed the results provided by processing the data. At least, on chapter 5, are grouped the conclusions.

Chapter 2.

General Concepts

Generally, the propagation effects on a wireless channel are:

Channel = path loss + static shadowing + dynamic shadowing + fading

all expressed in dB. In this chapter are explained each of this effects.

2.1. Path Loss

The path loss (or path attenuation) is the reduction of the power of an electromagnetic wave as it propagates through space, i.e. the ratio of the transmitted power to the received power between a pair of antennas situated at different positions, usually expressed in decibels (dB) [2].

It includes all of the possible elements of loss associated with interactions between the propagating wave and any objects between transmit and receive antenna, and may be due to many effects as free-space loss, refraction, diffraction, reflection, absorption... Path loss is also influenced by the environment (rural, urban, heavy urban...), the status of the propagation medium (air) and the distance between the transmitter and receiver.

The path loss is hard to measure directly because various losses and gains in the radio system have to be considered but is a major component in the analysis and design of the link budget of a telecommunication system.

The simplest useful form for an empirical path loss is as follows:

$$\frac{P_R}{P_T} = \frac{1}{L} = \frac{k}{r^n} \tag{1}$$

or in decibels

$$L = \eta \cdot 10\, log_{10} r + K \tag{2}$$

Where P_T and P_R are the effective isotropic transmitted and predicted isotropic received powers, L is the path loss, r is the distance between the transmitter and receiver antenna and k and η are constants.

Path loss is usually represented in dB and a more convenient form is

$$L = L_0 + \eta \cdot 10\, log_{10}\left(\frac{r}{r_0}\right) \quad (3)$$

where L_0 is the predicted loss at a reference distance r_0, usually 1 meter.

The parameter η is known as path loss exponent whose value is normally in the range of 2 to 4 [2] [4] and is dependent on the frequency and the system parameters, such as the environment. When the value is less than 2 means that there is a tunnel acting like a waveguide, when this value is higher than 4 means that we are in a lossy environment.

2.2. Shadowing

The channel is also affected by shadowing. The shadowing can be expressed by the addition of two terms: static shadowing and dynamic shadowing.

2.2.1. Static Shadowing

In the definition of the Path Loss is said that is a function only of parameters such environment, frequency and distance. The predicted path loss for a system operated in a particular environment will therefore be constant for a given distance as is defined in (3).

In practice, however, the particular clutter (walls, furniture…) along a path (link) at a given distance will be different for every path, causing variations respect to the nominal value given by the path loss models. For this reason some paths (links) will suffer more losses than other that are less obstructed and have increased signal strength.

This propagation effect is called shadowing or slow fading. The function of shadowing is a zero-mean with a log-normal distribution, i.e. the signal measured in dB has a normal distribution.

Moreover, the static shadowing is the time-invariant mean shadowing and estimated for a particular link as the difference between the time-averaged received power predicted by the deterministic path loss dependence and the time-averaged received power on the considered link.

For mobile and static links, static shadowing is related to the time-invariant obstructions of the links due to, for example, walls, furniture... and these obstructions differ for each link.

For static links, there is an additional interpretation of static shadowing. This is related to the frequency-selective fading, which has the same origin than space-selective fading, and is due by the partial signal cancellation by itself caused by the constructive or destructive combination of coherent multipath signals. This constructive or destructive combination is due to the different phases of the multipath arrival signals which it is due, equivalently, to the reception of tones at different frequencies as if it was a slight change of position of the antenna [4].

Due the distinction between the types of mobility, we may write the static shadowing as the sum of two terms:

$$\bar{S} = \bar{S_0} + \bar{S_S} \qquad (4)$$

where the former is the time-invariant obstruction loss and the latter is the space/frequency selective fading that only exists for static links.

2.2.2. Dynamic Shadowing

Represented by the variable *S(t)* in dB, it consists in the slow temporal variation of the received power around its static mean caused by the mobility of scatterers such as people, or of stations themselves.

Also known as shadow fading, slow fading or log-normal fading [5].

The difference between static shadowing and dynamic shadowing is that the static shadowing is related to time-invariant obstructions of the link such as furniture, and dynamic shadowing is related to the obstruction of mobile scatterers such as people walking or the mobility of the stations themselves and is time-variant.

When we analyze the signal over the time we can see that the fast fading (small-scale fading) and slow fading (dynamic shadowing) are integrated. The slow fading is like the envelope that the fast fading signal follows, i.e. is the average over the small-scale fading. It can be done by averaging the envelope or magnitude of the Rx signal over distance (e.g. 10m) or using a sliding window spanning [5].

In the Figure 1.2.1. we show a signal over time,

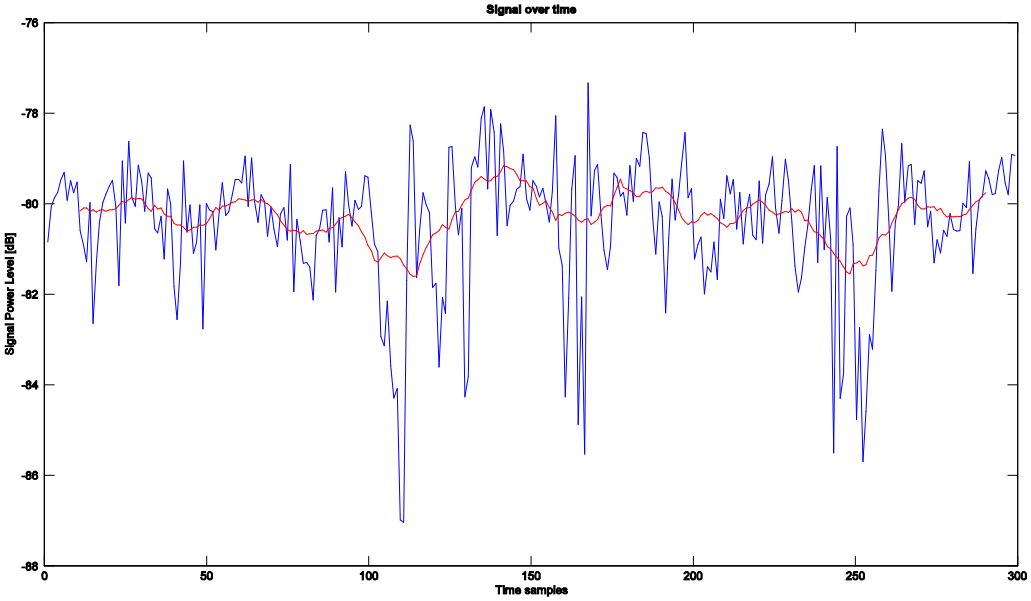

FIGURE 1.2.1. SIGNAL OVER TIME

the blue curve is the signal power level in dB and we can see the fast fading (small-scale fading). The red curve is the average over the small-scale fading using a moving window spanning.

2.3. Fading

The fading is the variation of the attenuation that a signal experiences over certain propagation media. In radio communications, the fading may vary with the position of the antenna, the frequency and/or with time. This fading may be due to multipath propagation, referred as small-scale fading or fast fading, or due to shadowing from obstacles affecting the wave propagation, referred as shadow fading or slow fading.

The slow fading is caused by movement over distances large enough to produce gross variations in the overall path between the transmitter and receiver or as the result of obstruction by mobile scatterers such as people or objects [3]. The dynamic shadowing explained in 2.2.2. represents the slow fading.

The classical small-scale fading or fast fading is denoted as *r(t)* in natural scale and it is due by the local multipath interference, i.e. the coherent constructive or destructive combination of the multipath arrival signals, resulting from the small-scale motions of the stations and/or environment [4]. It is observed over distances of about half a wavelength. We can observe this behaviour in the Figure 1.2.1., where the variations induced in the blue curve are due by the small-scale fading or fast fading.

In the measurements the small-scale fading is present when the antennas were moving in both ends or in just one end, or for the nomadic case when the environment affected.

The small-scale fading behaviour can be characterized by Ricean, Rayleigh, Nakagami or Weibull distributions. Rayleigh and Ricean distributions are the most common used. Is it considered too another distribution called Double-Rayleigh. In the next paragraphs there are explained the mentioned fading behaviours:

- ***Ricean**:* It occurs when in multipath one signal is stronger than the others, i.e. the presence of a non-fading or coherent component, and could be caused when there is LOS. Concretely, for mobile scenarios the coherent contribution is often associated with the LOS component. In fixed scenarios many scattered contributions are coherent, as transmitter, receiver and scenario are static, only a few scattered contributions are non-coherent. The amplitude gain is characterized by a Ricean distribution. The channel is complex Gaussian with non-zero mean. Ricean pdf can be written as

$$p_{Rice}(r) = \frac{r}{\sigma^2} e^{-\left(\frac{r^2}{2\sigma^2}+K\right)} I_0\left(r\frac{\sqrt{2K}}{\sigma}\right) \quad (5)$$

  The K-factor is the relation between the power of the LoS component (coherent part) and the power of the Rayleig component (non-coherent part) [4][5].

- ***Rayleigh**:* when the components of the channel are independent the pdf of the amplitude has Rayleigh pdf.

$$p_{Rayleigh}(r) = \frac{r}{\sigma^2} e^{-\left(\frac{r^2}{2\sigma^2}\right)} \quad (6)$$

  The Rayleigh fading is the particular case of Ricean fading for K=0. This is the most used signal model in wireless communications and the worst fading case although it can be found worst cases called Double-Rayleigh [4][5]. The Double-Rayleigh distribution is as follows:

$$p_{DR}(r) = \frac{r}{\sigma^4} K_0\left(\frac{r}{\sigma^2}\right) \quad (7)$$

  Where $K_0(\cdot)$ is a zeroth ordered modified Bessel Function of the second kind [10].

Chapter 3.

Process

In this chapter is explained the process to obtain the results from the data. The process is the same that was done in [4].

In SISO configuration there are 8 transmitter antennas (Tx) and 8 receiver antennas (Rx), hence there are 64 (8x8) possible links. Of this 64 possible links are discarded those that have a low signal-to-noise ratio (SNR), i.e. lower than 10dB. The number of links discarded is different for each mobile scenario.

There is a distinction among link mobility types:

- ***Static or nomadic*:** all the nodes of the link, transmitter and receiver, are static.
- ***Single-mobile*:** one node of the link is mobile and the other is static.
- ***Double-mobile*:** all the nodes of the link are mobile.

Each type of mobility has a different data treatment.

Static links

As the space-selective fading and frequency-selective fading are caused by the combination of multipath signals, as explained in the previous chapter, the whole frequency is divided into 60 sub-bands of 2 frequency tones each sub-band except the last sub-band that contains 3 tones because we have a total of 121 frequency tones.

$$F_{sub} = 2\ tones/subband$$

To calculate the average received power for each sub-band in each link

$$P[b, tx, rx] = \frac{1}{F_{sub} \cdot T} \sum_{t=1}^{T} \sum_{f=1+(b-1)F_{sub}}^{bF_{sub}} |H[t, f, tx, rx]|^2 \qquad (8)$$

that it is to average the power within each sub-band over all time samples. Where *b*=1…60, *tx*=1…8, *rx*=1…8 and *T*=300 in our case.

The average power over all frequency sub-bands for each link is

$$P[tx, rx] = \frac{1}{N_{sub}} \sum_{b=1}^{N_{sub}} P[b, tx, rx] \quad (9)$$

where N_{sub} is the number of sub-bands equal to 60 in our case and *P[b,tx,rx]* is the average received power for each sub-band.

Mobile links

For mobile links, time, space and frequency-selective fading share the same cause, i.e. the motion of the node causes phase shifts in each multipath. Hence, the fading statistics over time at a given frequency are similar to the statistics over frequency at any given time.

For this reason, it is not necessary to treat time and frequency on a separate basis and to divide the whole frequency band. We only care for the results that equation (9) gives us to obtain the received power. Recombining equation (8) and (9) we obtain a function that calculates the average received power over all time and frequency samples

$$P[tx, rx] = \frac{1}{T \cdot F} \sum_{t=1}^{T} \sum_{f=1}^{F} |H[t, f, tx, rx]|^2 \quad (10)$$

Where *T*=300 and *F*=121 in our case.

3.1. Path Loss

The path-loss and static shadowing is modelled expressing the received power $P|_{dB}$ at a distance *d* from the transmitter as

$$P|_{dB}(d) = P_0|_{dB} - \eta \cdot 10 \log_{10}\left(\frac{d}{d_0}\right) - \bar{S} - n_{wi} \cdot L_{wi} \quad (11)$$

where $P_0|_{dB}$ is the signal power at the reference distance d_0, usually 1 meter in I2I scenarios.

The individual path loss L is defined as

$$L = \Lambda_0 + \eta \cdot 10\log_{10}\left(\frac{d}{d_0}\right) + \bar{S} + n_w \cdot L_w \qquad (12)$$

where Λ_0 is the deterministic path-loss at a reference distance d_0 and $\bar{S}$ is the static shadowing.

Denote that the attenuation of the walls is considered to calculate the path-loss, where n_{wi} is the number of walls of a particular type and L_{wi} is the attenuation of each wall for this particular type, isolating it from the static shadowing and the deterministic path-loss. The types of walls are:

- Thin walls composed of plasterboard.
- Thick walls composed of bricks.

This consideration is taken in other models like COST 231 [2].

The equation (11) is used to do the fitting process to obtain the path-loss exponent parameter η, and the attenuation factor L_{wi} of each type of wall.

3.2. Static shadowing

The ***obstruction shadowing*** S_o, that is a part of static shadowing, is determined as the difference between the observed power *P[tx,rx]* and the deterministic average power that we obtain with the fitting function. The distribution of S_o is lognormal, i.e. characterized by the mean μ_{So} and standard deviation σ_{So}.

The ***spatial fading*** S_s, the other part of static shadowing, only exists for static channels. The spatial fading is the difference between the average power for each link and the power on each frequency sub-band, i.e. for each link we obtain 60 samples of spatial fading according to the frequency sub-bands. As spatial fading is a fading factor, we consider the best treatment using SOSF (Second-Order Scattering Fading distribution) that gives the variation of the power and which type of fading is following by the static links for all scenarios, this distribution is used in [4]. The fading distributions considered in SOSF are Ricean, Rayleigh and Double-Rayleigh.

The SOSF distribution can be specified by two parameters α and β constrained to the triangle $\alpha \geq 0, \beta \geq 0, \alpha + \beta = 1$.

When α = 0 consists in a Ricean fading, when $\alpha = \beta = 0$ is a Rayleigh fading and when α = 1 and β = 0 is a Double-Rayleigh fading.

3.3. Dynamic Shadowing

As is said in the previous chapter, the dynamic shadowing is represented by the variable *S(t)* in dB and consists in the slow temporal variation of the received power around its static mean over the time caused by the mobility of scatterers such as people, or of stations themselves.

To do the average over the small-scale fading, a moving spanning window with amplitude of 20 time samples is taken. This value is chosen because fits well to static, single-mobile and double-mobile links and gets out a good average. Therefore, small-scale fading is averaged out, while still following the slow variations induced by the motion of people, or by station moving in the environment.

Denote that the 16s scenario is not considered because in this scenario the links are static but the environment too, and we do not have any kind of dynamic shadowing. Therefore, we only use the scenarios with some part mobile, environment or nodes. These scenarios are 16sp, 16ms, 16mLs and 16rms.

The span of the sliding window corresponds to

$$T_{av} = 20\ [time\ samples] \cdot \frac{1}{2.65\ [Hz]} = 7.5472\ s \qquad (13)$$

where 2.65Hz is the effective burst rate and therefore a time sample is equal to

$$\frac{1}{2.65\text{Hz}} = 0.3774\text{s}$$

The average over small-scale fading is done by

$$Ps[t,b,l] = \frac{1}{F_{sub}T_{av}} \sum_{t'=t-\frac{T_{av}}{2}}^{t+\frac{T_{av}}{2}-1} \sum_{f=1+(b-1)F_{sub}}^{bF_{sub}} |H[t',f,l]|^2 \qquad (14)$$

A third dimension array *Ps[t,b,l]* is used considering the time, the subbands and each link. The subband dimension allows us to see that the dynamic shadowing is frequency-independent.

Finally, we obtain the dynamic shadowing *S[t,b,l]* as the variation of *Ps|dB* around its mean,

$$S[t,b,l] = P_s|_{dB} - E\{P_s|_{dB}\} \quad (15)$$

where *E{…}* denotes the expectation value over time axis.

The ***dynamic shadowing autocorrelation*** is also found to follow a negative exponential. The model parameters are therefore the standard deviation σ_S, estimated using the sample variance, and the slope τ of the temporal autocorrelation [4],

$$R_S(\Delta t) = \frac{E\{S(t)S(t+\Delta t)\}}{\sigma_S^2} = e^{-\frac{\Delta t}{\tau}} \quad (16)$$

The slope of the temporal autocorrelation is the time that must pass to change the dynamic shadowing. For mobile links, the slope τ may also be expressed as the ratio of a decorrelation distance d_c to an effective speed *v*, corresponding to the motion of the nodes.

As there are a lot of links (8x8), the dynamic shadowing may be highly correlated between these, which significantly affect the performance in distributed networks. Estimating the ***correlation coefficients*** between links (l) and (l') by

$$C\ [b,l,l'] = \frac{\sum_{t=1}^{T} S[t,b,l]S[t,b,l']}{\sqrt{\sum_{t=1}^{T} S[t,b,l]^2 \sum_{t=1}^{T} S[t,b,l']^2}} \quad (17)$$

These correlation coefficients are evaluated between all links in one measurement. The resulting correlation values are then grouped in different sets:

1. links with a common Rx (denoted as 'Rx')
2. links with a common Tx (denoted as 'Tx')
3. links with a common Rx or a common Tx (union of sets 1 and 2, denoted as 'Rx-Tx')
4. links with no node in common (complement of set 3, denoted as 'disjoint')
5. all links (union of sets 3 and 4, denoted as 'all')

For every set, is calculated the mean, the standard deviation, the minimum, and the maximum value of correlation coefficients.

3.4. Fading

The small scale fading is described by the received signal amplitude, *r*. The normalization of each channel is done by its respective power, the power considered to find the dynamic shadowing.

$$G\,[t, f, l] = \frac{H[t, f, l]}{\sqrt{P_s[t, [f / F_{sub}], l]}} \tag{18}$$

The signal amplitude is $r = |G|$. *r* it's a parameter depending on the time, frequency and link.

The best treatment to characterize the fading behavior is using SOSF (Second-Order Scattering Fading) distribution used also in [4]. The fading distributions considered in SOSF are Ricean, Rayleigh and Double-Rayleigh. SOSF distribution can be specified by two parameters α and β constrained to the triangle $\alpha \geq 0, \beta \geq 0, \alpha + \beta = 1$. These parameters correspond to the Double-Rayleigh component and the LOS component respectively. When $\alpha = 0$ consists in a Ricean fading, when $\alpha = \beta = 0$ is a Rayleigh fading and when $\alpha = 1$ and $\beta = 0$ is a Double-Rayleigh fading.

When the SOSF distribution program is executed, the input parameters are *[t x f]* samples for each link. But to see how the fading behaviour varies in time per link we divide the time in bins obtaining 14 bins of 20 samples of time in each.

Predicting the fading behaviour in nomadic case follows a Ricean distribution, is obtained the *K* parameter for each link and frequency and then is obtained the relation between the parameter *K* and the link distance.

In the mobile case there is a distinction between single and double mobile.

Chapter 4.

Results

In this section there are the results obtained doing the process of the previous chapter over all the data.

4.1 Path Loss and Static Shadowing

There are four models defining the parameters that the fitting function takes into account:

- ***Model 1***: Just contemplating the path loss exponent η.
- ***Model 2***: Contemplating the path loss exponent and the attenuation of walls L_w, without distinction between thick (brick) and thin (plasterboard) walls.
- ***Model 3***: Contemplating the path loss exponent η and the attenuation of walls, distinguishing the types of walls, thick L_{thick} or thin L_{thin}.
- ***Model 4***: Contemplating the path loss exponent and the attenuation of walls, only taking into account thick walls.

The parameters in tables are those explained above. The results for each model are the following:

4.1.1. Tables

4.1.1.1. Static links

Model 1

	16 - s	16 - sp	16 - ms	16 - mLs	16 - rms	All scenarios
η	6,0139	6,0585	6,6407	6,5368	6,6197	**6,1954**
μ_{So} [dB]	0	0	0	0	0	**0**
σ_{So} [dB]	6,2503	6,361	7,1568	6,8482	6,9833	**6,4706**

TABLE 1.4.1. PATH LOSS AND STATIC SHADOWING MODEL 1 (STATIC LINKS)

Model 2

	16 - s	16 - sp	16 - ms	16 - mLs	16 - rms	All scenarios
η	5,5474	5,5717	4,5849	4,7956	4,6387	**5,3399**
L_w	0,8542	0,8126	3,1366	2,6566	3,0226	**1,4315**
μ_{So} [dB]	0	0	0	0	0	**0**
σ_{So} [dB]	6,2164	6,3242	6,7548	6,5488	6,601	**6,3717**

TABLE 1.4.2. PATH LOSS AND STATIC SHADOWING MODEL 2 (STATIC LINKS)

Model 3

	16 - s	16 - sp	16 - ms	16 - mLs	16 - rms	All scenarios
η	5,4091	5,2032	4,5388	4,4746	4,5404	**5,1921**
L_{thick}	1,833	2,4835	3,3647	2,9026	3,5092	**2,4365**
L_{thin}	0	0	2,8425	2,3391	2,3953	**0,4347**
μ_{So} [dB]	0	0	0	0	0	**0**
σ_{So} [dB]	6,1171	6,0839	6,7467	6,5391	6,5635	**6,2477**

TABLE 1.4.3. PATH LOSS AND STATIC SHADOWING MODEL 3 (STATIC LINKS)

Model 4

	16 - s	16 - sp	16 - ms	16 - mLs	16 - rms	All scenarios
η	5,409	5,2032	5,6829	5,6874	5,5047	**5,3602**
L_{thick}	1,8331	2,4834	2,0945	1,8573	2,4386	**2,2484**
μ_{So} [dB]	0	0	0	0	0	**0**
σ_{So} [dB]	6,1171	6,0839	6,9771	6,7008	6,7324	**6,2544**

TABLE 1.4.4. PATH LOSS AND STATIC SHADOWING MODEL 4 (STATIC LINKS)

When the attenuation of the thin walls (model 3) is considered, this parameter is not taken in account in all the scenarios, only for the 16-ms, 16-mLS and 16-rms. When the fitting is done for all the scenarios together, this value is practically zero. For this reasons this model is discarded.

Comparing the model 2 and 4, the model 4 is more 'realistic' because take more into account the attenuation of walls. In the model 2 the attenuation value is quite low. In [6] [7] the attenuation of a brick wall at 2.4GHz is approximately 4-6dB. However, this attenuation varies between 2dB and 3dB and we cannot fix the attenuation value to obtain the path loss exponent parameter.

Almost all η parameters given by the four models and for all scenarios are between 5 and 6 dB, which is a η value acceptable for an office scenario as it is seen in others experiments with similar characteristics [8].

The obstruction shadowing is zero-mean as it is expected and its standard deviation, named location variability, is around 6,3dB which means that there is not a significant variation. In the scenarios where is present the small range movement the standard deviation is higher. The location variability parameter influences in the coverage, the larger the location variability, the lower the coverage range [2].

Figure 1.4.1. shows the alpha-beta relation that SOSF fitting gives us for all static links in all distributed scenarios. The most of the static links present a Double-Rayleigh fading, this could be related to the quantity of scatterers around the transmitter and the receiver. Figure 1.4.2. shows the fitting error histogram. In Figure 1.4.3. it is represented the alpha-beta relation vs the distance of each link. The spatial fading is independent of the distance.

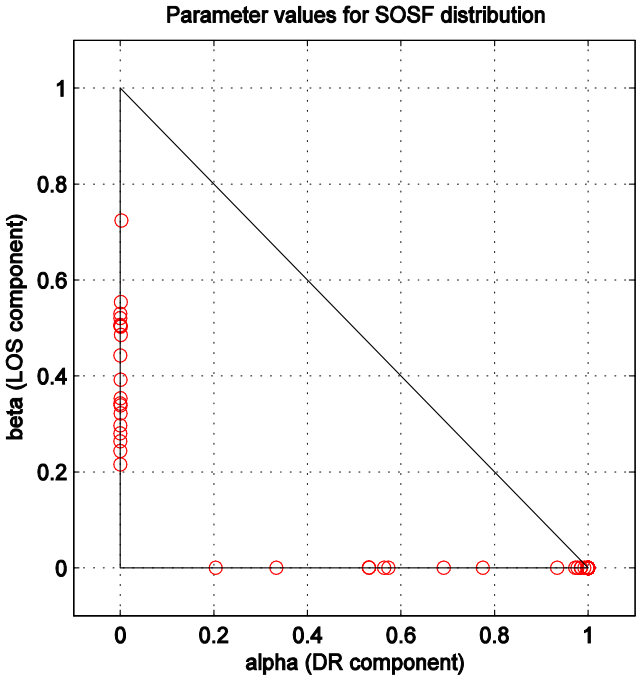

FIGURE 1.4.1. ALPHA-BETA RELATION FOR STATIC LINKS

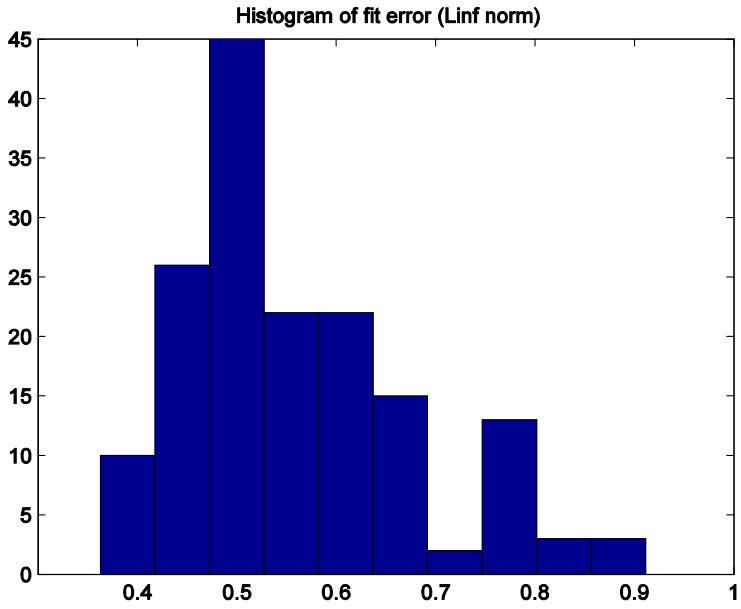

FIGURE 1.4.2. FITTING ERROR HISTOGRAM

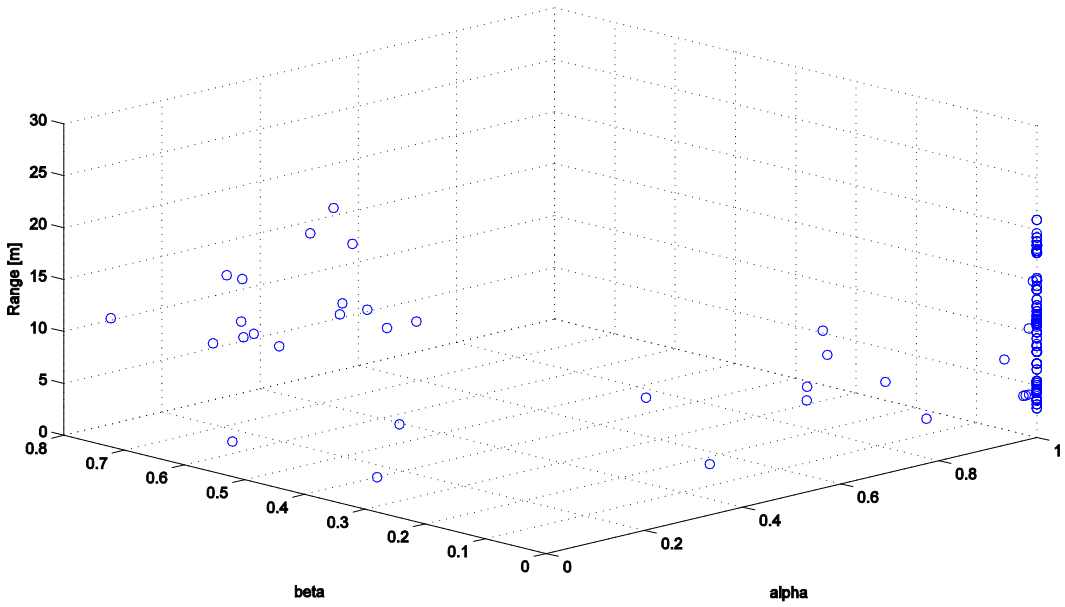

FIGURE 1.4.3. ALPHA-BETA RELATION VS DISTANCE

Figure 1.4.4. is an example of obstruction shadowing shape and in Figure 1.4.5. a fitting of its distribution.

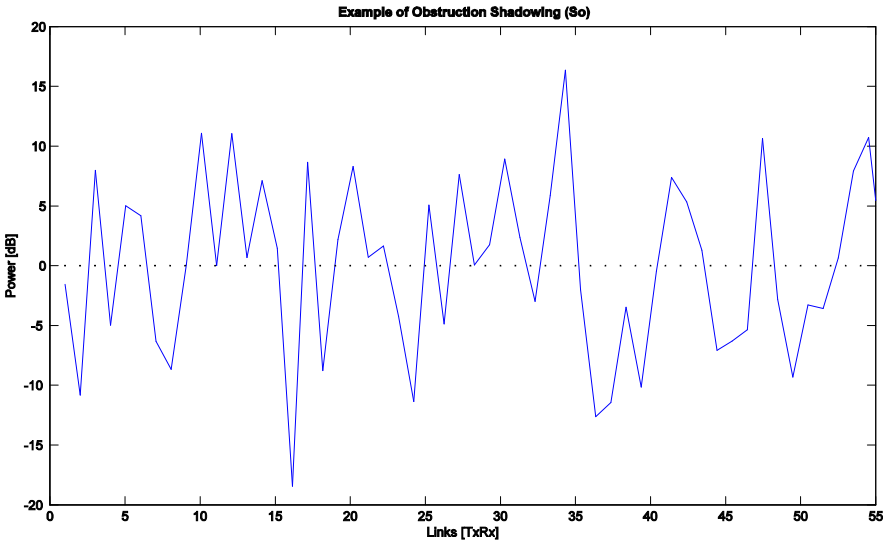

FIGURE 1.4.4. OBSTRUCTION SHADOWING

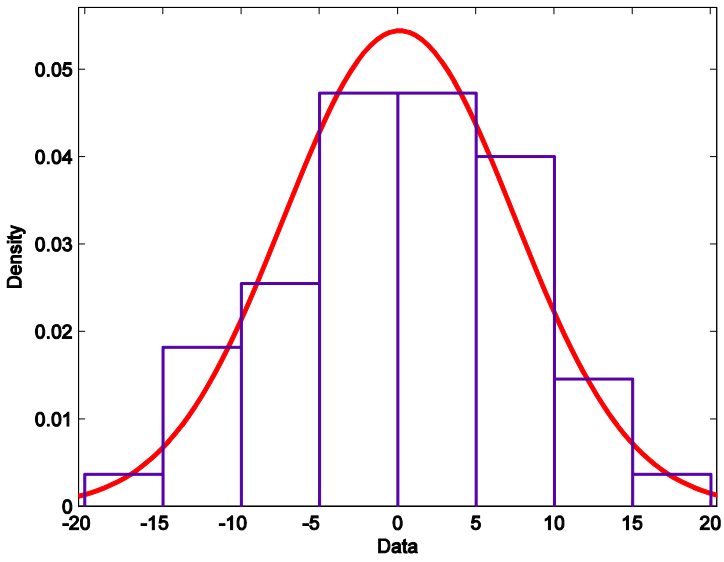

FIGURE 1.4.5. DISTRIBUTION OF OBSTRUCTION SHADOWING

4.1.1.2. Mobile links

Model 1

	16 - ms	16 - mLs	16 - rms	All scenarios
η	5,9728	5,9807	5,1185	**5,7666**
μ_{So} [dB]	0	0	0	0
σ_{So} [dB]	4,9592	5,9206	7,1347	**6,0119**

TABLE 1.4.5. PATH LOSS AND STATIC SHADOWING MODEL 1 (MOBILE LINKS)

Model 2

	16 - ms	16 - mLs	16 - rms	All scenarios
η	4,9403	4,6924	5,0205	**4,887**
L_w	1,7053	2,1025	0,1667	**1,4569**
μ_{So} [dB]	0	0	0	0
σ_{So} [dB]	4,7332	5,6356	7,1332	**5,878**

TABLE 1.4.6. PATH LOSS AND STATIC SHADOWING MODEL 2 (MOBILE LINKS)

Model 3

	16 - ms	16 - mLs	16 - rms	All scenarios
η	4,7631	4,5304	3,9657	**4,657**
L_{thick}	3,073	3,3231	3,7346	**3,1696**
L_{thin}	0,7797	1,2403	0	**0,3177**
μ_{So} [dB]	0	0	0	0
σ_{So} [dB]	4,5149	5,4864	6,6066	**5,6055**

TABLE 1.4.7. PATH LOSS AND STATIC SHADOWING MODEL 3 (MOBILE LINKS)

Model 4

	16 - ms	16 - mLs	16 - rms	All scenarios
η	5,0847	5,042	3,9653	**4,7881**
L_{thick}	2,7613	2,8325	3,7346	**3,0406**
μ_{So} [dB]	0	0	0	0
σ_{So} [dB]	4,5532	5,5641	6,6066	**5,6107**

TABLE 1.4.8. PATH LOSS AND STATIC SHADOWING MODEL 4 (MOBILE LINKS)

The η values are a little low than the static nodes case. In the 16-rms scenario this value is significantly lower. The behaviour of the wall attenuation is very similar than the static links,

the values are around 3dB. The fitting in Model 3 do not take into account the attenuation of thin walls because this value is almost zero.

The obstruction shadowing is zero-mean. Its standard deviation is lower than in static links, but in 16-rms scenario is a little higher.

4.1.2. Graphics

The following figures are the graphics within the data and the different fitting functions, classified by the different scenarios:

4.1.2.1. Scenario 16-s

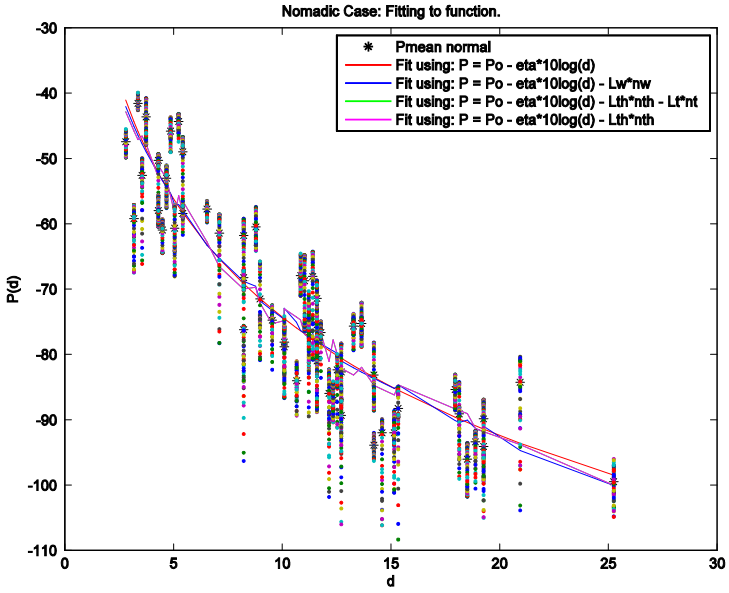

FIGURE 1.4.6. PATH LOSS FITTING - SCENARIO 16S (STATIC LINKS)

4.1.2.2. Scenario 16-sp

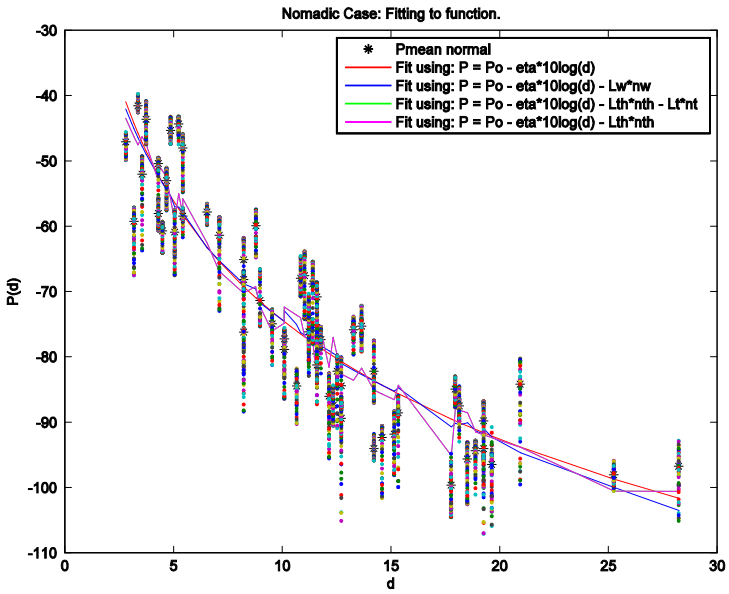

FIGURE 1.4.7. PATH LOSS FITTING - SCENARIO 16SP (STATIC LINKS)

4.1.2.3. Scenario 16-ms

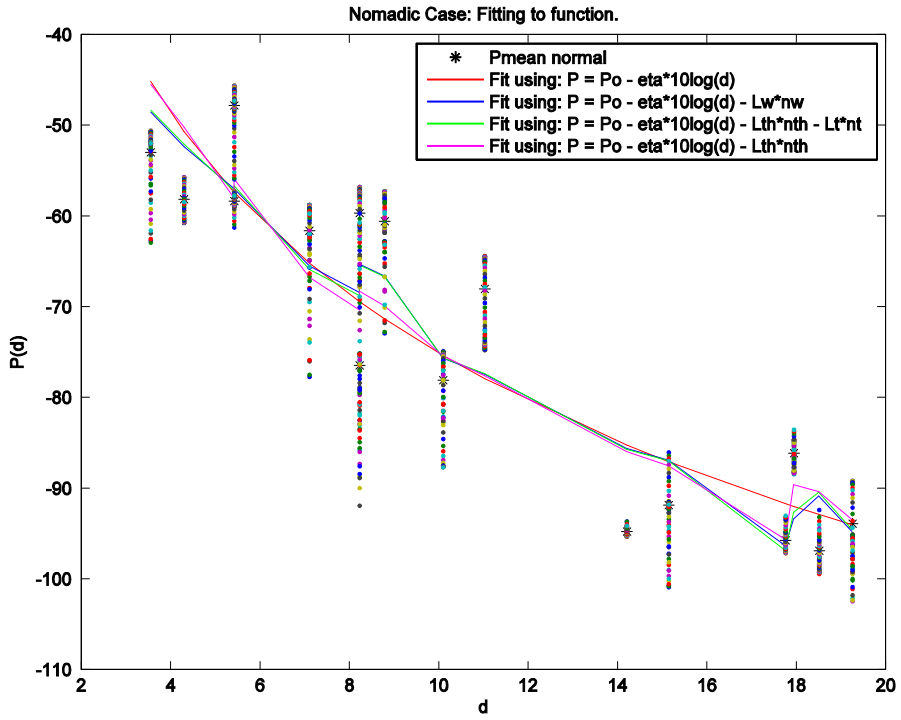

FIGURE 1.4.8. PATH LOSS FITTING - SCENARIO 16MS (STATIC LINKS)

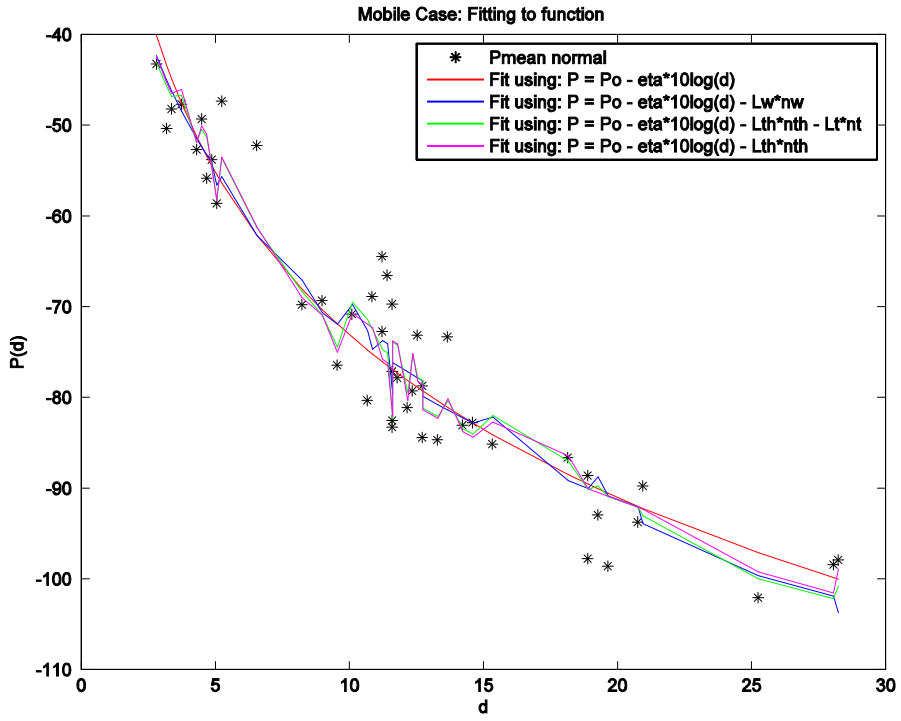

FIGURE 1.4.10. PATH LOSS FITTING - SCENARIO 16MS (MOBILE LINKS)

4.1.2.4. Scenario 16-mLs

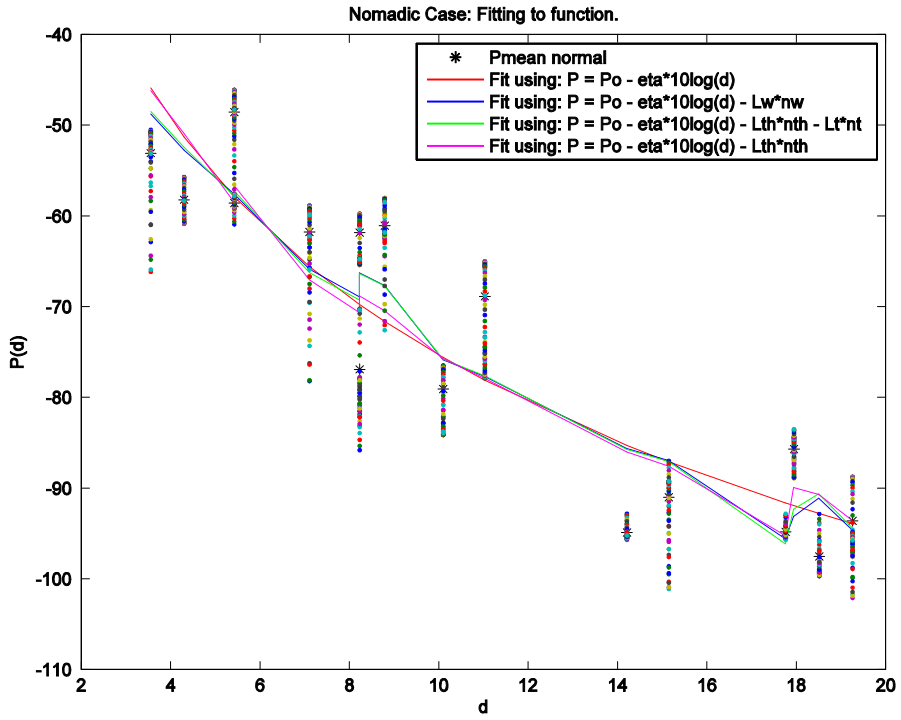

FIGURE 1.4.11. PATH LOSS FITTING - SCENARIO 16MLS (STATIC LINKS)

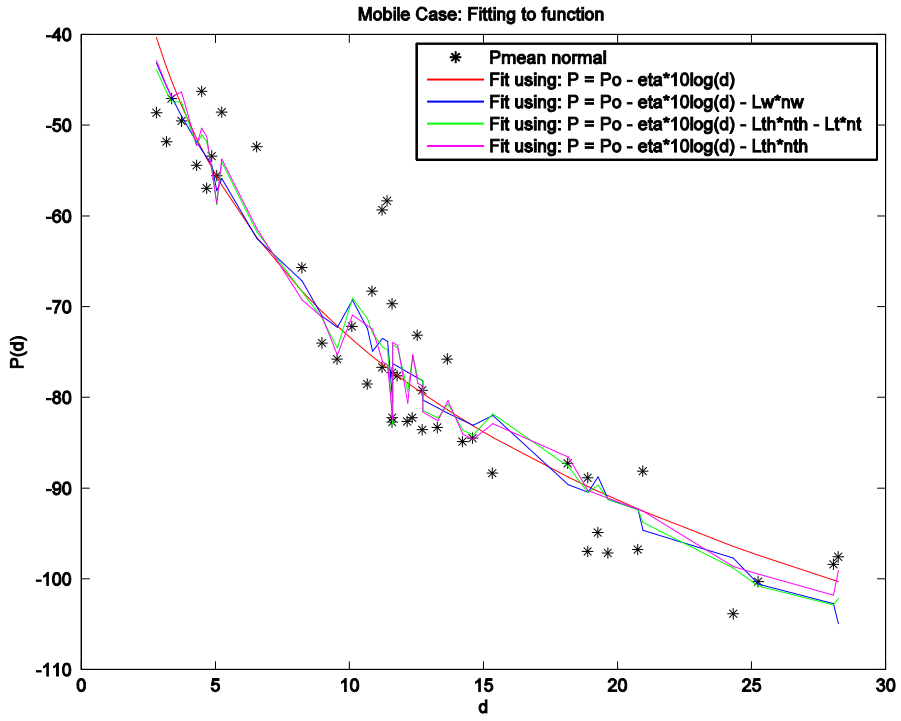

FIGURE 1.4.12. PATH LOSS FITTING - SCENARIO 16MLS (MOBILE LINKS)

4.1.2.5. Scenario 16-rms

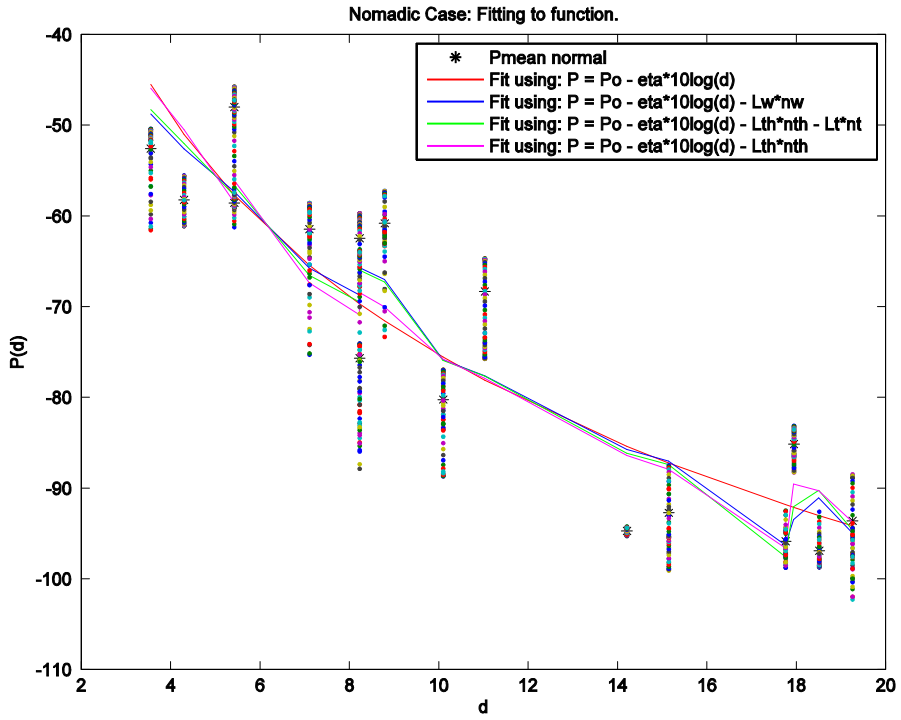

FIGURE 1.4.13. PATH LOSS FITTING - SCENARIO 16RMS (STATIC LINKS)

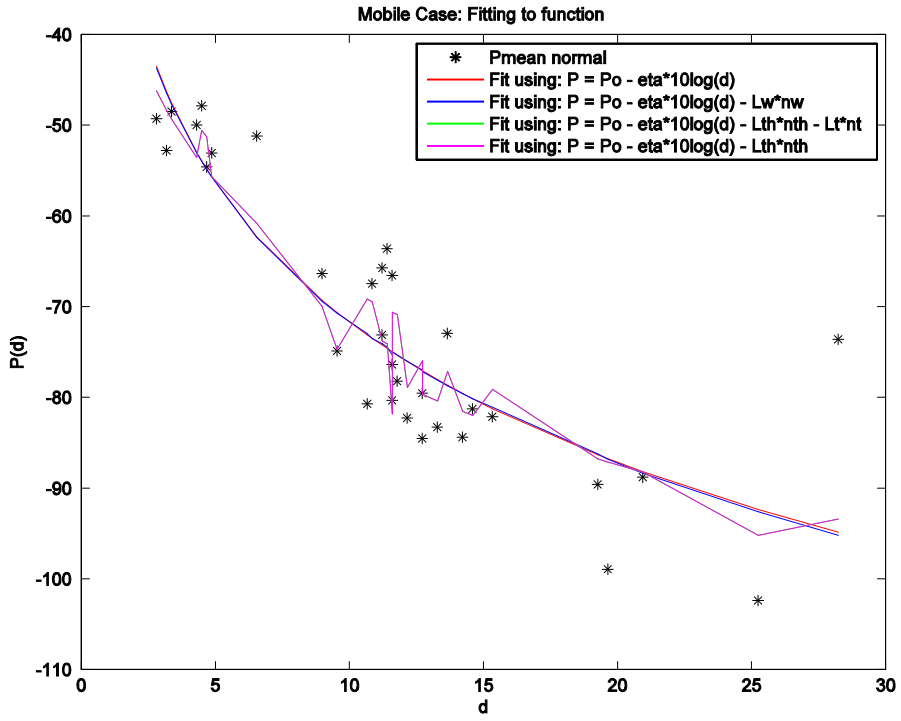

FIGURE 1.4.14. PATH LOSS FITTING - SCENARIO 16RMS (MOBILE LINKS)

4.1.2.6. All Scenarios

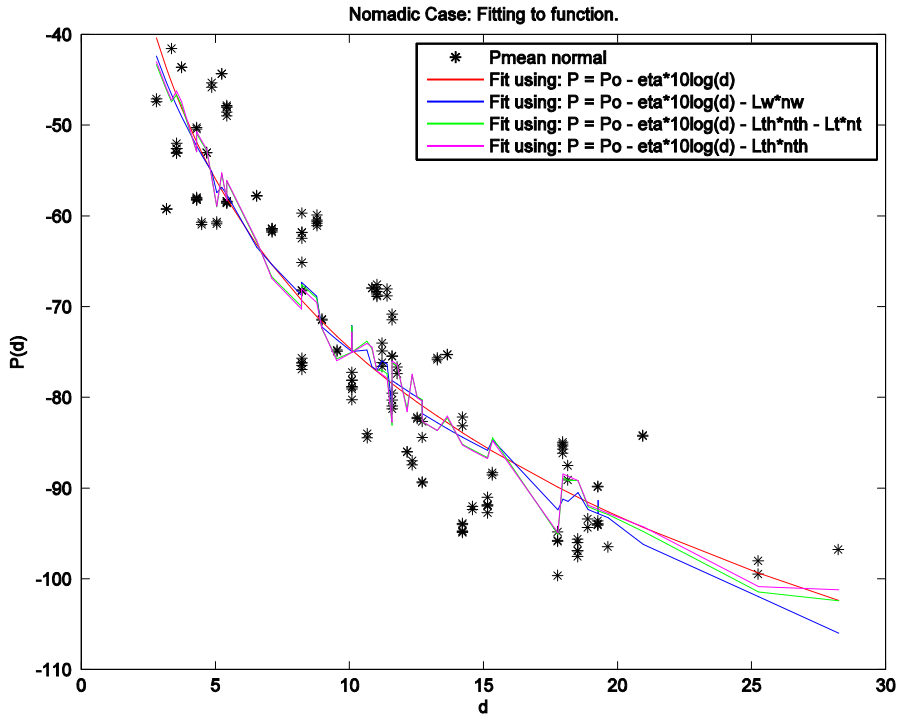

FIGURE 1.4.15. PATH LOSS FITTING - ALL SCENARIOS (STATIC LINKS)

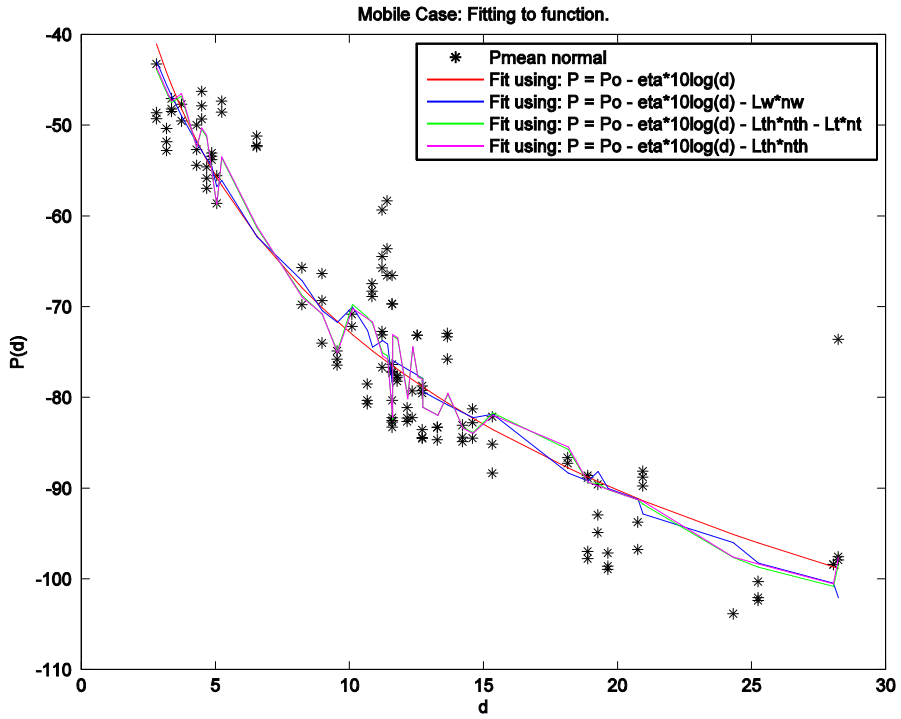

FIGURE 1.4.16. PATH LOSS FITTING - ALL SCENARIOS (MOBILE LINKS)

Finally, the following graphics show the contribution of the eta parameter in the power in the static and mobile cases.

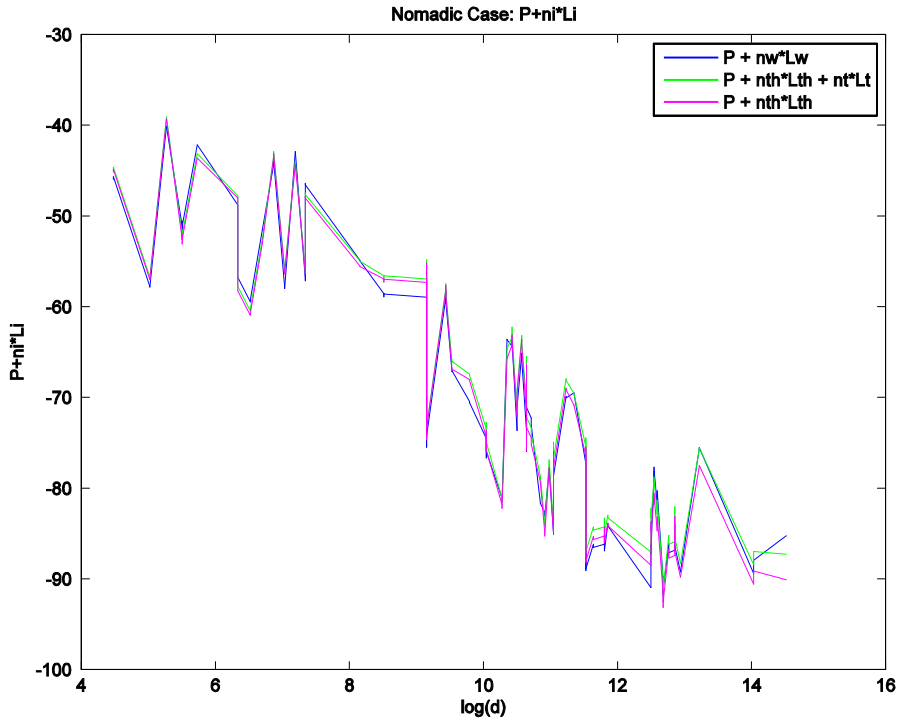

FIGURE 1.4.17. CONTRIBUTION ETA PARAMETER (STATIC LINKS)

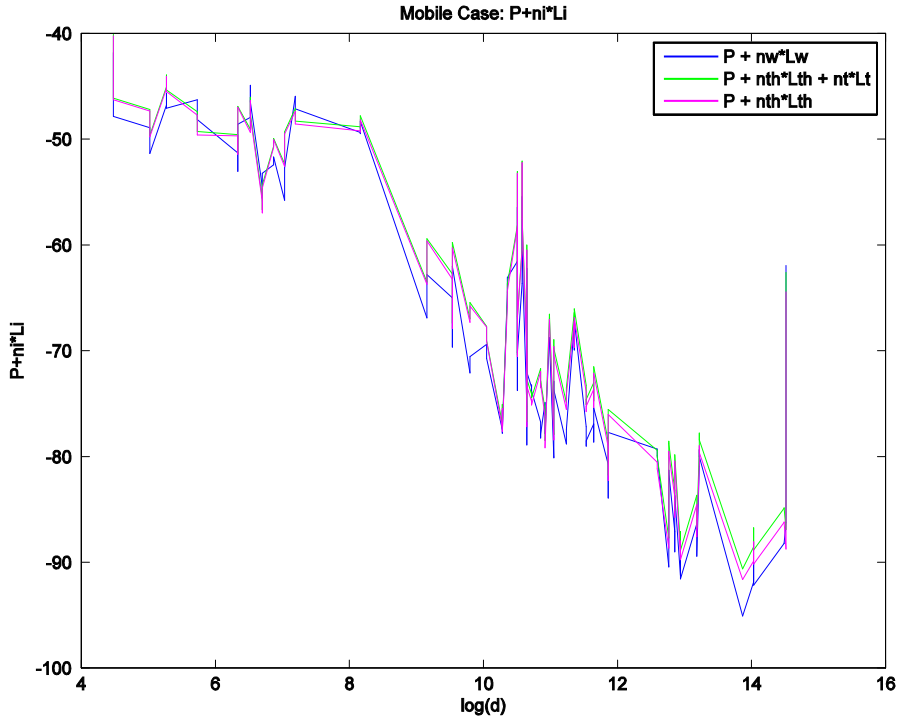

FIGURE 1.4.18. CONTRIBUTION ETA PARAMETER (MOBILE LINKS)

4.2 Dynamic Shadowing

The calculations have been made with different amplitudes of the moving spanning window (10 samples and 20 samples).

The data reveals that dynamic shadowing is frequency-independent, i.e. all the subband signals of the same link have more or less the same shape, as is shown in the next graph,

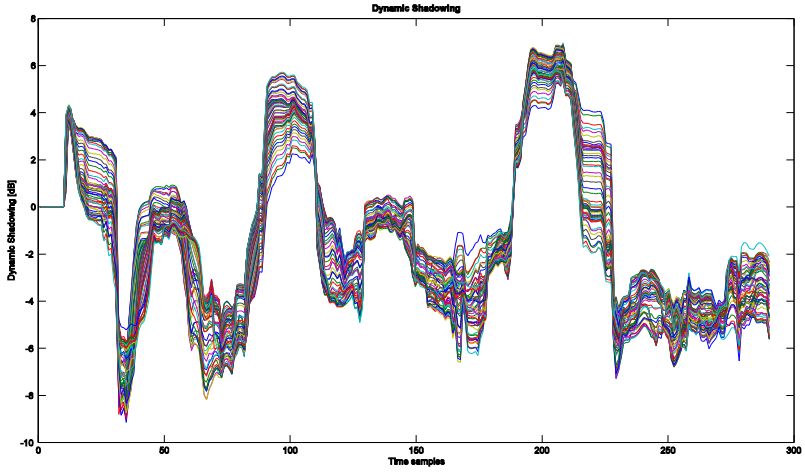

FIGURE 1.4.19. DYNAMIC SHADOWING SIGNAL OF ALL SUBBANDS

and log-normally distributed, i.e. S is Gaussian distributed, with a mean μ_S= 0 by definition.

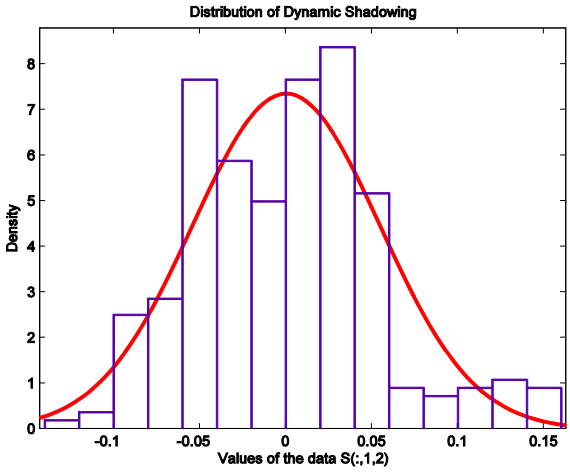

FIGURE 1.4.20. DISTRIBUTION OF DYNAMIC SHADOWING

We classified all the data considering the mobility type of the links (static, single-mobile or double-mobile). In the next graphs we can see the different behaviours of the signal in these three types of mobility where we can see that as higher mobility, higher signal fluctuations.

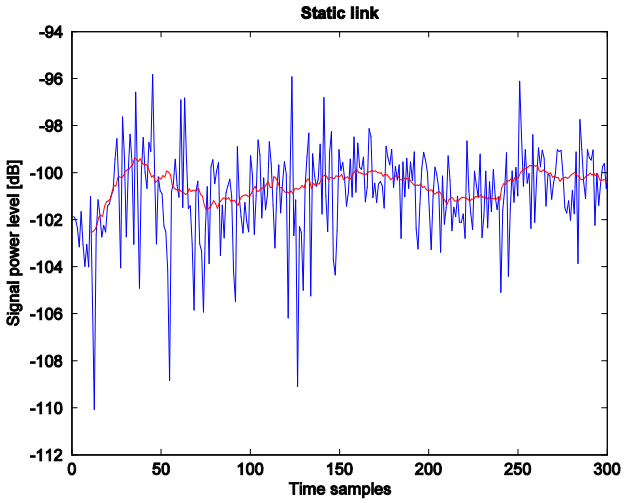

FIGURE 1.4.21. DYNAMIC SHADOWING OF STATIC LINK

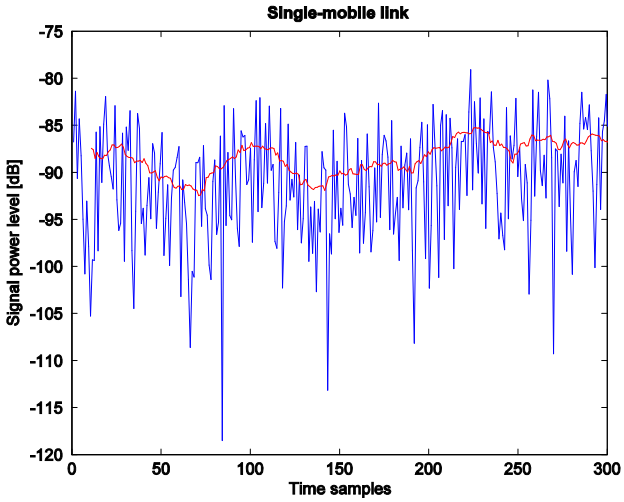

FIGURE 1.4.22. DYNAMIC SHADOWING OF SINGLE-MOBILE LINK

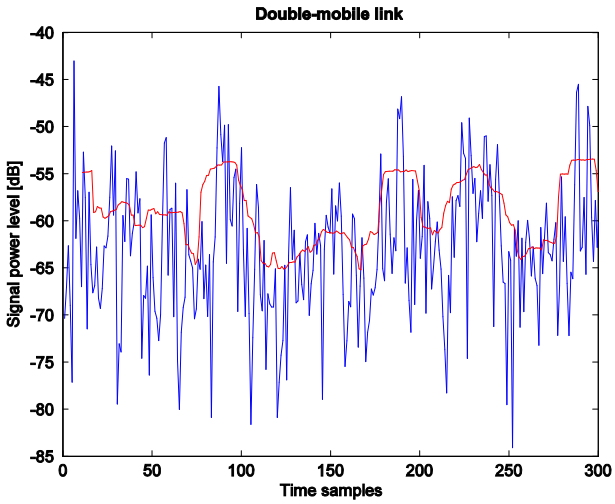

FIGURE 1.4.23. DYNAMIC SHADOWING OF DOUBLE-MOBILE LINK

4.2.1 Autocorrelation

In the next tables are shown the results of the slope of temporal autocorrelation $\tau[s]$. As it is explained in the process section, $\tau[s]$ is the time that must pass to change the dynamic shadowing.

For Tav=20 samples

	Static	Single Mobile	Double Mobile
τ[s]	4.7252	4.5361	5.8070

TABLE 1.4.9. SLOPE OF DYNAMIC SHADOWING TEMPORAL AUTOCORRELATION (20 SAMPLES)

And for Tav=10 samples

	Static	Single Mobile	Double Mobile
τ[s]	3.4309	3.8518	~~12.8674~~

TABLE 1.4.10. SLOPE OF DYNAMIC SHADOWING TEMPORAL AUTOCORRELATION (10 SAMPLES)

In Figure 1.4.24. is shown the distribution of shadowing autocorrelation for static, single mobile and double mobile links and its fitting.

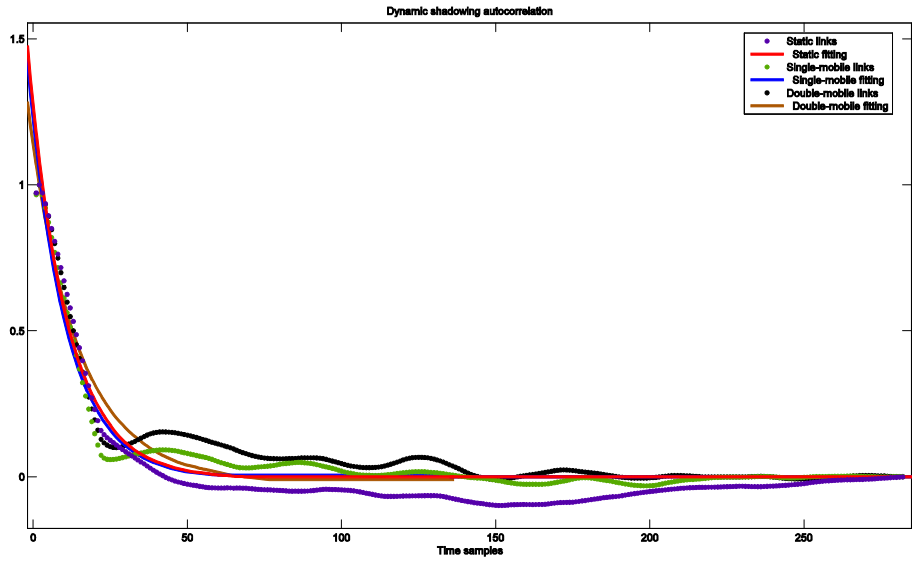

FIGURE 1.4.24. DYNAMIC SHADOWING TEMPORAL AUTOCORRELATION FITTING

The value of slope of temporal autocorrelation depends on the number of samples used to define the wide of the moving spanning window. The values of the static links are near the values for the single-mobile links. The value for double-mobile links is higher than the two before.

4.2.2. Cross-correlation

These are the correlation coefficients among links or cross-correlation coefficients. These results are for Tav=20 samples.

Scenario	Subset	Mean	Std.	Max	Min
I2I static	All	0.0135	0.1659	0.7165	-0.5812
	Rx	-0.0019	0.1895	0.5746	-0.5812
	Tx	0.0178	0.1718	0.7087	-0.3924
	Rx-Tx	0.0078	0.1811	0.7087	-0.5812
	Disjoint	0.0155	0.1603	0.7165	-0.4864
I2I double mobile	All	0.1519	0.2348	0.9847	-0.4490
	Rx	0.1903	0.2623	0.8414	-0.2273
	Tx	0.1471	0.2375	0.6778	-0.4490
	Rx-Tx	0.1687	0.2507	0.8414	-0.4490
	Disjoint	0.1407	0.2232	0.9847	-0.3786
I2I single mobile (Rx)	All	0.1149	0.2677	0.9509	-0.5048
	Rx	0.2388	0.2986	0.9398	-0.4704
	Tx	0.0651	0.1970	0.6234	-0.3748
	Rx-Tx	0.1519	0.2670	0.9398	-0.4704
	Disjoint	0.0905	0.2656	0.9509	-0.5048
I2I single mobile (Tx)	All	0.0764	0.2245	0.7571	-0.4852
	Rx	0.0449	0.1573	0.3368	-0.2895
	Tx	0.2015	0.3113	0.7571	-0.4852
	Rx-Tx	0.1232	0.2583	0.7571	-0.4852
	Disjoint	0.0453	0.1932	0.6128	-0.3740

TABLE 1.4.11. DYNAMIC SHADOWING CROSS-CORRELATION COEFFICIENTS (20 SAMPLES)

And for Tav = 10 samples

Scenario	Subset	Mean	Std.	Max	Min
I2I static	All	0.0137	0.1381	0.7216	-0.4845
	Rx	0.0001	0.1578	0.5106	-0.4845
	Tx	0.0137	0.1444	0.6354	-0.3569
	Rx-Tx	0.0069	0.1514	0.6354	-0.4845
	Disjoint	0.0161	0.1331	0.7216	-0.4415
I2I double mobile	All	0.2001	0.2002	0.9789	-0.3571
	Rx	0.2301	0.2299	0.8049	-0.1715
	Tx	0.1999	0.2063	0.7112	-0.3571
	Rx-Tx	0.2150	0.2186	0.8049	-0.3571
	Disjoint	0.1901	0.1865	0.9789	-0.2309
I2I single mobile (Rx)	All	0.1498	0.2182	0.9336	-0.3485
	Rx	0.2676	0.2382	0.9218	-0.2598
	Tx	0.0995	0.1398	0.5410	-0.2134
	Rx-Tx	0.1836	0.2123	0.9218	-0.2598
	Disjoint	0.1276	0.2195	0.9336	-0.3485
I2I single mobile (Tx)	All	0.1217	0.1861	0.7510	-0.3986
	Rx	0.0928	0.1185	0.3773	-0.1744
	Tx	0.2427	0.2745	0.7510	-0.3986
	Rx-Tx	0.1677	0.2239	0.7510	-0.3986
	Disjoint	0.0914	0.1490	0.4910	-0.2286

TABLE 1.4.12. DYNAMIC SHADOWING CROSS-CORRELATION COEFFICIENTS (10 SAMPLES)

The most significant values are marked in red. In double-mobile links there are high values in all the cases, i.e. when the node in common is the receiver (Rx), the node in common is the transmitter (Tx) and when neither is common. In single-mobile links we have high values when the mobile antenna, regardless of whether the transmitter or receiver, is that which the nodes have in common. The other values are practically zero.

Comparing these results of correlation with those obtained in [4]:

- The behaviour is similar in single-mobile nodes, i.e. we have high values when the nodes have the mobile antenna in common.
- In double-mobile links we also have high values when we have some node in common (Tx or Rx). But in our case we have high values when no node is in common (disjoint), while in [4] this value is practically zero.
- In static nodes the behaviour is similar. All values are practically zero.

4.2.3. Standard deviation

The Figure 1.4.25. represents the standard deviation of dynamic shadowing versus the individual path loss for nomadic scenarios.

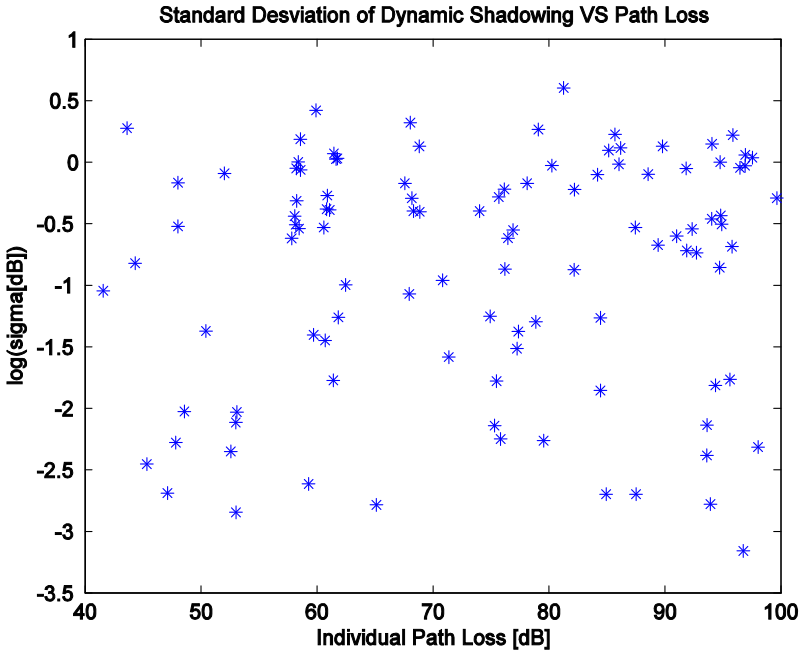

FIGURE 1.4.25. STD DYNAMIC SHADOWING VS PATH LOSS

Unfortunately, the correlation between the path loss and the standard deviation of dynamic shadowing cannot be extracted.

The distribution of the standard deviation of dynamic shadowing is a normal distribution

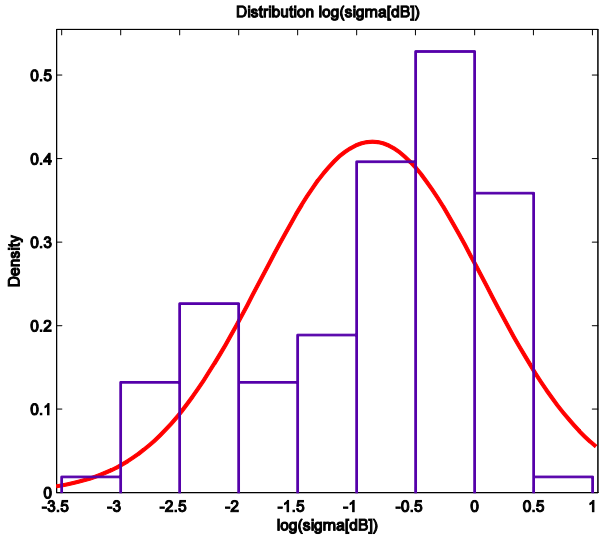

FIGURE 1.4.26. STD DYNAMIC SHADOWING DISTRIBUTION

the mean value of the distribution is around -0.85 and it's standard deviation is 0.94.

4.3 Fading

4.3.1. Static Nodes

For almost all the links the fading behaviour is characterized by Ricean distribution when $\alpha = 0$ and $\beta > 0$ as is shown in Figure 1.4.27.

The fading behaviour for the static links varies along the time. In Figure 1.4.28. are shown some links that do not change on time and another link where factor *K* changes as the beta changes, $K = \beta/(1-\beta)$.

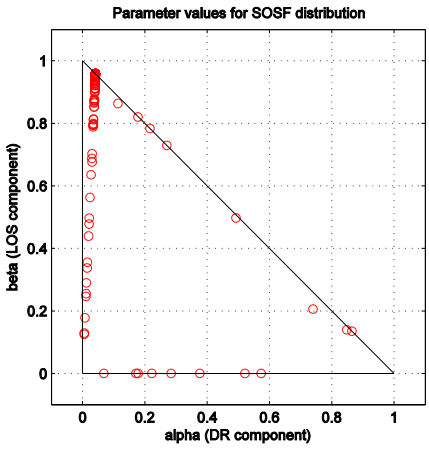

FIGURE 1.4.27. FADING BEHAVIOUR IN STATIC LINKS

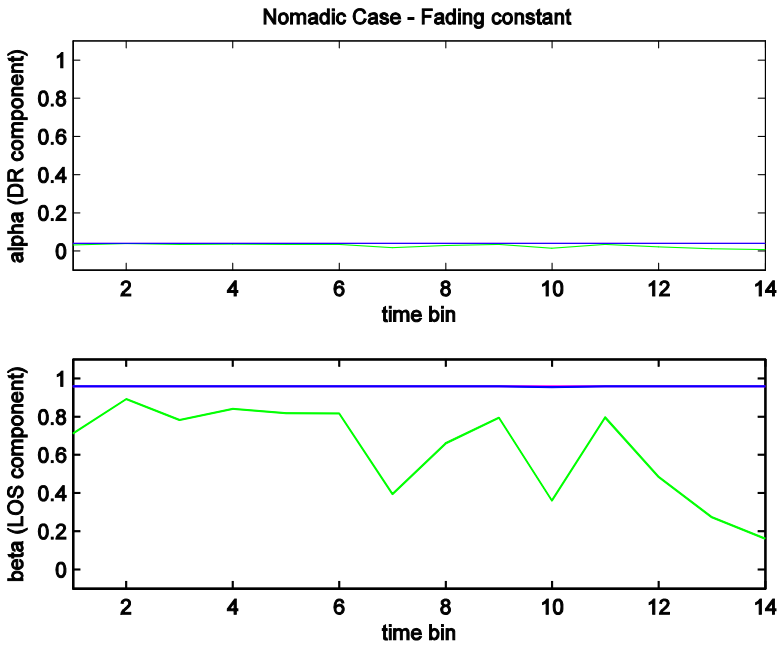

FIGURE 1.4.28. LINKS WHERE FADING IS PRACTICALLY CONSTANT ALONG THE TIME

In Figure 1.4.29. is shown the fading behaviour of three links that vary from Ricean to Double Rayleigh.

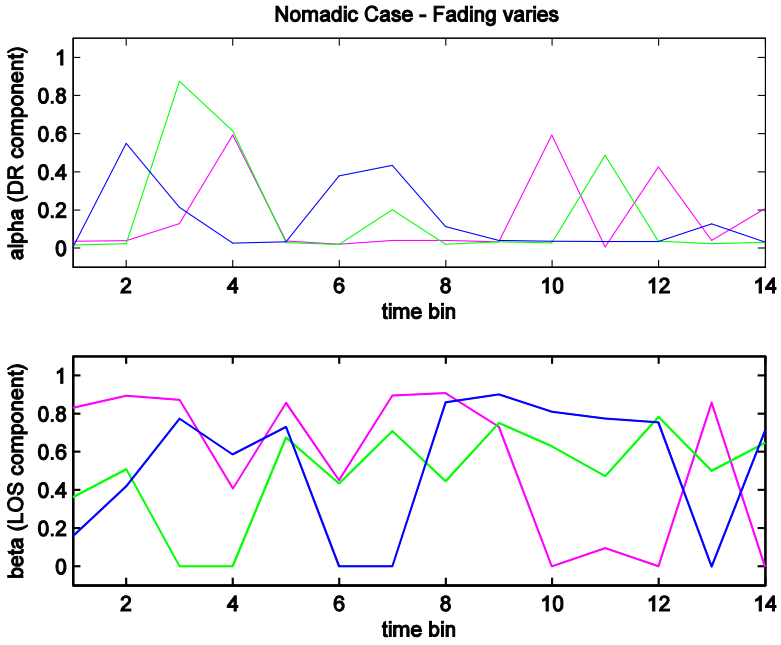

FIGURE 1.4.29. LINKS WHERE FADING VARIES ALONG THE TIME

As the fading behaviour of the static links is characterized by a Ricean distribution, in Figure 1.4.30. is shown the relation between the *K* factor of each link and the link distance. This can be fitted by

$$K\big|_{dB} = 21.72 - 2.08\log_{10}(\frac{d}{d_0}) + \sigma'_K \qquad (19)$$

Where *d* is the link distance in meters and σ'_K is approximately a random Gaussian variable of standard deviation equal to 3.8 dB. The *K-factor* decreases with the distance increasing.

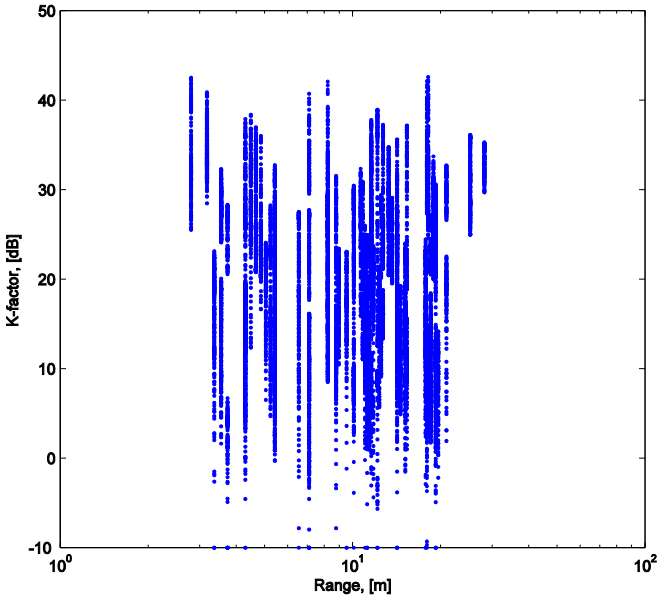

FIGURE 1.4.30. K-FACTOR VS DISTANCE

4.3.2. Mobile Nodes

In both the single and double mobility cases, the Double-Rayleigh distribution is present as is shown in Figure 1.4.31. and Figure 1.4.32.

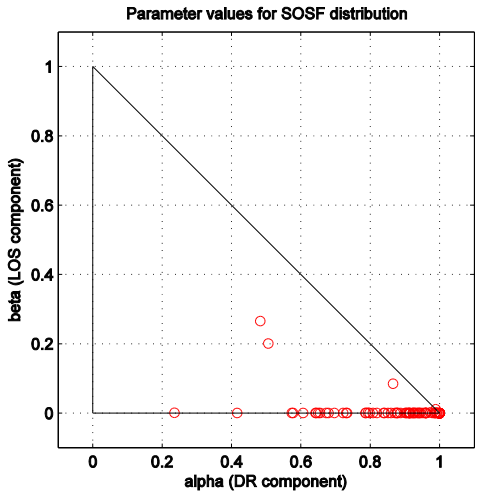

FIGURE 1.4.31. FADING BEHAVIOUR IN SINGLE-MOBILE LINKS

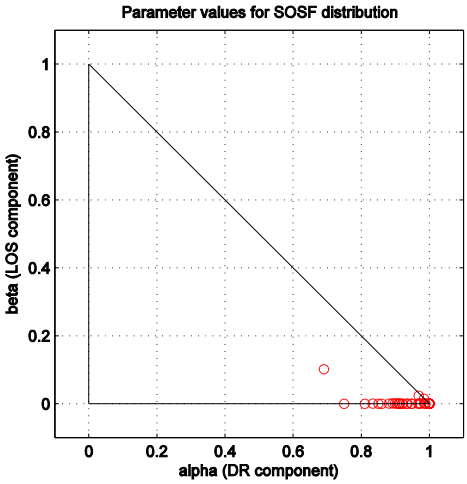

FIGURE 1.4.32. FADING BEHAVIOUR IN DOUBLE-MOBILE LINKS

In single mobile and double mobile there are pure Double Rayleigh (DR) channels, Figure 1.4.33. and Figure 1.4.34., what means that the fading behaviour is practically almost all the time DR.

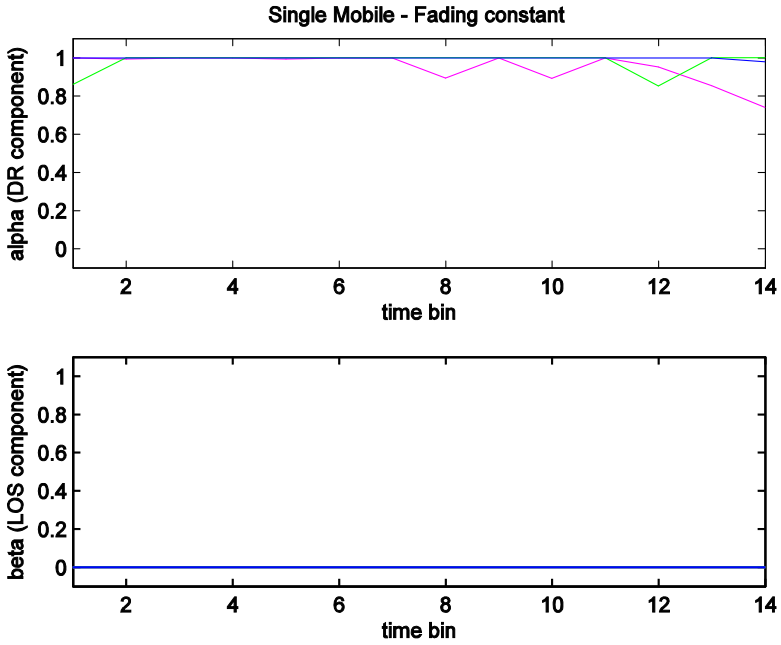

FIGURE 1.4.33. SINGLE-MOBILE LINKS WHERE FADING IS PRACTICALLY CONSTANT ALONG THE TIME

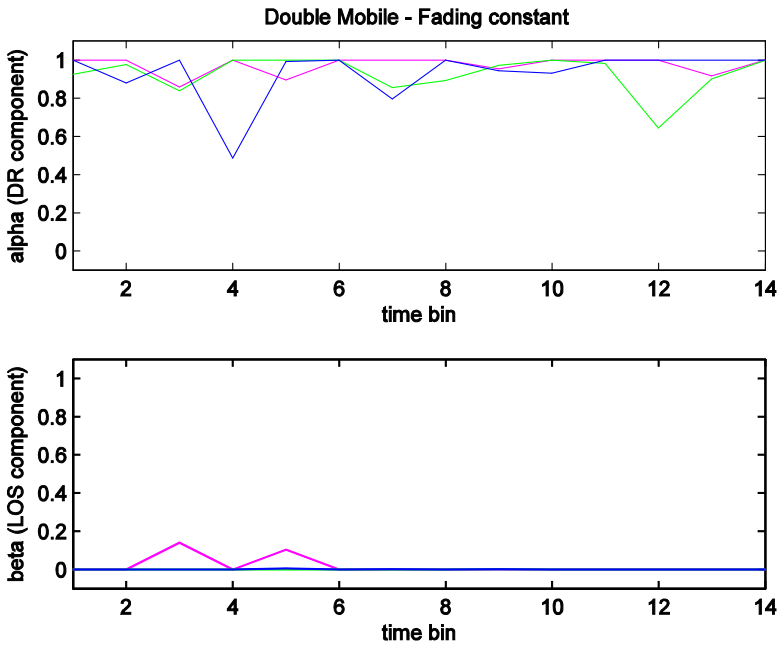

FIGURE 1.4.34. DOUBLE-MOBILE LINKS WHERE FADING IS PRACTICALLY CONSTANT ALONG THE TIME

There are other links where its fading behaviour changes from Ricean to Double Rayleigh passing by Rayleigh in time as is shown in Figure 1.4.35. and Figure 1.4.36.

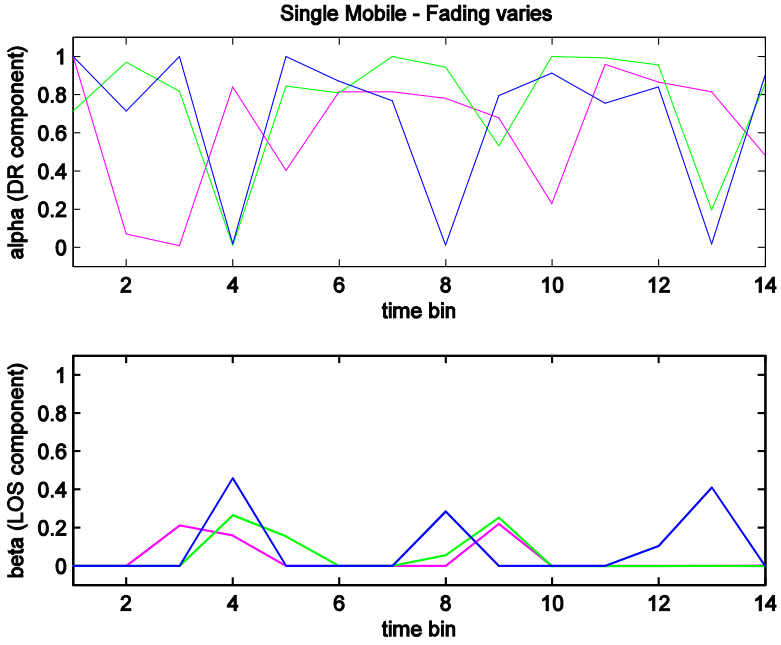

FIGURE 1.4.35. SINGLE-MOBILE LINKS WHERE FADING VARIES ALONG THE TIME

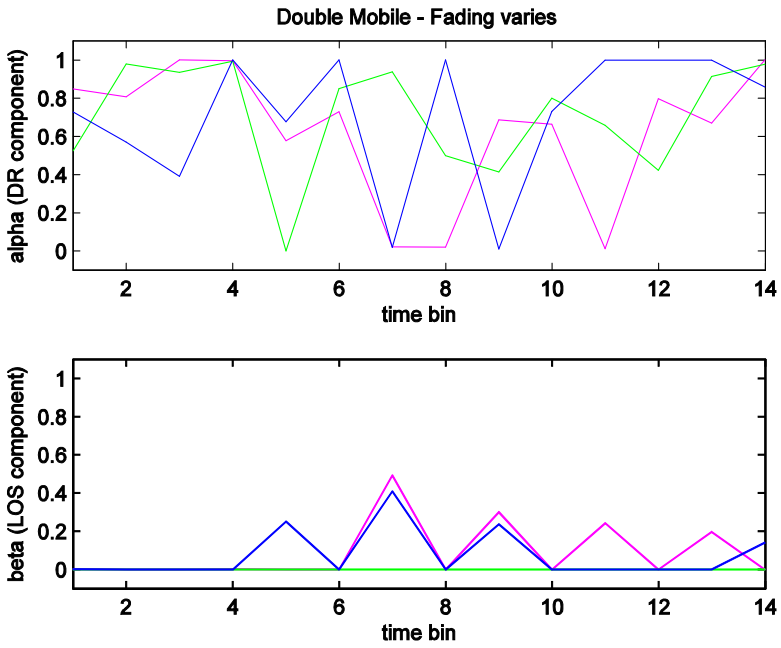

FIGURE 1.4.36. DOUBLE-MOBILE LINKS WHERE FADING VARIES ALONG THE TIME

4.4. Model parameters

	Nomadic	Single-Mobile	Double-Mobile
η	5.36	4.79	
L_w [dB]	2.25	3.04	
μ_{So} [dB]	0	0	
σ_{So} [dB]	6.25	5.61	
(α_S,β_S)	Fig. 1.4.1.	-	
σ_S [dB]	Fig. 1.4.25.	-	
τ [s]	4.72	4.53	5.8
K	See (19)	non-applicable	
(α,β)	Fig. 1.4.26.	Fig. 1.4.30.	Fig. 1.4.31.

TABLE 1.4.18. SISO MODEL PARAMETERS

Chapter 5.

Conclusions

This part has presented an analysis and modelling of indoor-to-indoor channels based on experimental results. There are the main conclusions:

- The analysis is based on a wideband experimental campaign at 3.8 GHz.
- We separate the static and the mobile nodes to find the different factors involved. The static shadowing for the static nodes includes also spatial fading, which models the static multipath interference.
- To do the fitting of the path loss and static shadowing we used four different models which contemplate the attenuation of the different types of walls.
- Of the four models we choose the fourth one, which considers the eta parameter and the attenuation of the thick walls. We choose it because presents for any scenario and any link type a low standard deviation value of the obstruction shadowing σ_{SO} that means is the best fitting error if we think the obstruction shadowing is the difference between the fitted curve and the data.
- Almost all η parameters given by the four models and for all scenarios are between 5 and 6 dB in static nodes and between 4 and 6 dB for mobile nodes, which is an η value acceptable for an office scenario as it is seen in others experiments with similar characteristics.
- The wall attenuation is between 2 and 3 dB.
- The standard deviation of the static obstruction shadowing for all scenarios for static nodes is about 6.3 dB. For the mobile nodes is a little low, around 5.6 dB.
- The distribution of the spatial fading most present in static links is the Double-Rayleigh distribution, this could be related to the quantity of scatterers around the transmitter and the receiver.
- The slope of the temporal autocorrelation $\tau[s]$ in dynamic shadowing is higher for double-mobile links than for single-mobile and static links, that are practically equal.
- The cross-correlation coefficients for double-mobile links are high in all the cases, i.e. when the node in common is the transmitter or the receiver or when there is no node

in common. In single-mobile links we have high values when the mobile antenna, regardless of whether the transmitter or receiver, is that which the nodes have in common. In nomadic nodes the values are practically zero.

- We did not found a correlation between the standard deviation of dynamic shadowing and the path loss.

- For nomadic scenarios, small-scale fading is characterized by Ricean distribution and the K-factor decrease with increasing distance.

- For mobile scenarios, both double-mobile and single-mobile nodes fading behaviour is characterized by Double-Rayleigh distribution.

PART 2.

Multiple Antenna Analysis (MIMO)

Chapter 1.

Introduction

Since the first transmission via radio, the wireless communications have suffered an evolution. The objective of this evolution is to transmit much information, as far away, in the shortest time, with the best quality and at the lowest cost possible.

Actually, due to the age of the information, there are high requirements in the speed transmission and in quality of the communications. As we said in the previous part, great progresses have been realized in modulation, codification and signal processing to maximize the spectral efficiency with the purpose of covering these necessities. But this spectral efficiency is limited by the Shannon capacity and the spectre of radio is a limited resource with bandwidths fixed and finite. Also the radio channel is a hostile environment that degrades the quality of the communications.

The use of multiples antennas in transmission and reception, in fact space-time (ST) or Multiple-Input Multiple-Output (MIMO) systems, offers significant increases in spectral efficiency, coverage, speed transmission and link reliability without additional bandwidth or transmit power.

But these systems also add more complexity in the transmitter and reception stages as a heavy reliance on radio channel characteristics. The scattering richness of the scenario is a key factor to the decorrelation of the subchannels generated among transmitter and receiver antennas. As in the traditional systems, the spatial correlation among channels causes a decrease of the gain produced by the use of multiples antennas.

For all these reasons, MIMO is a current theme of international wireless research.

Chapter 2.

General concepts

2.1. Introduction

As is said before, MIMO systems is a promising technology to achieve high transmission speeds without additional bandwidth or transmitted power. In contrast with SISO systems, the scattering and the delay dispersion leads to increase the transmission rates.

The *spatial diversity* is a widely used technique in the reception end to improve the channel performance, as increases the signal-to-noise ratio. The spatial diversity in the transmitter is realized by the space-time coding or with the spatial multiplexing (SM). The *space-time coding* aims to improve the reliability and the quality of the channel, reducing the bit error rate (BER). The *spatial multiplexing (SM)* transmits several information fluxes by the different transmitter antennas. In the reception end, these fluxes are divided through signal processing increasing the spectral efficiency.

The use of multiples antennas in transmission and reception leads to the generation of independent and parallel sub-channels which gain is determined by the eigenvalues of the *Wishart matrix* (HH^H). The magnitude of these eigenvalues depends on the channel characteristics and the antennas used. These values are useful to characterize de MIMO channel.

If the *channel status* is known at the transmitter, an efficiently transmit is possible by distributing properly the power using a technique known as water-filling. If the channel status is unknown by the transmitter, the power distribution among antennas is realized uniformly hence less effectively.

The MIMO channel performance is measured through the *channel capacity*, i.e. the maximal spectral efficiency that the channel offers. The channel capacity only depends on the signal to noise ratio in the reception end and on the channel matrix, independently of the transmission or encoding scheme used. Spatial multiplexing uses the spatial domain to obtain high speed transmission rates, close to the channel capacity. The space-time coding is aimed to improve the reliability and quality of the channel, i.e. transmitting and receiving several replicas of the same symbol.

The *spatial correlation*, as in the classic systems, is a factor that specifies the MIMO channel performance, reducing the capacity.

2.2. Antenna configurations

In the next figure there are the different antenna configurations for ST wireless links.

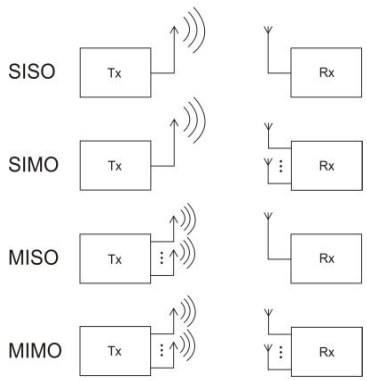

FIGURE 2.2.1. SCHEME OF ANTENNA CONFIGURATIONS IN A MIMO SYSTEM

- **SISO** *(Single Input Single Output)* is the classic wireless configuration.
- **SIMO** *(Single Input Multiple Output)* has a single transmitter antenna and multiple receive antennas (M_R).
- **MISO** *(Multiple Input Single Output)* has multiple transmitter antennas (M_T) and single receive antenna.
- **MIMO** *(Multiple Input Multiple Output)* has multiple transmitter antennas (M_T) and multiple receive antennas (M_R).

The MIMO-MU (MIMO multiuser), and evolution of the MIMO configuration, is a configuration that refers to the case where a base-station with multiple antennas communicates with P users each with one or more antennas. Can be seen as the extended concept of space-division multiple access (SDMA) which allows a terminal to transmit (or receive) signal to (or from) multiple users in the same band simultaneously.

2.3. Channel matrix

In a MIMO system with M transmitter antennas and N receiver antennas, MxN system, MN sub-channels are generated between the transmitter array and the receiver array. The impulse response in a narrowband MIMO channel is expressed as:

$$H(t) = \begin{pmatrix} h_{11}(t) & h_{12}(t) & \cdots & h_{1M}(t) \\ h_{21}(t) & h_{22}(t) & \cdots & h_{2M}(t) \\ \vdots & \vdots & \ddots & \vdots \\ h_{N1}(t) & h_{N2}(t) & \cdots & h_{NM}(t) \end{pmatrix} \quad (20)$$

Each of the elements $h_{ij}(t)$ represents a channel generated between the transmitter antenna j (j=1,...,M) and the receiving antenna i (i=1,...,N).

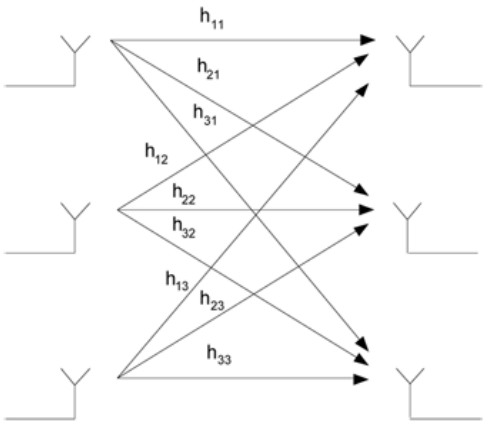

FIGURE 2.2.2. SCHEME OF SUBCHANNELS GENERATED IN A MIMO SYSTEM

2.4. Basis of MIMO systems

The high transmission speed in MIMO systems depends on various factors that improves the transmission schemes or improves the channel reliability.

2.4.1. Spatial multiplexing gain

Spatial multiplexing offers a linear (in the number of transmit-receive antenna pairs or $\min(M_R,M_T)$) increase in the transmission rate or capacity for the same bandwidth and with no additional power expenditure.

2.4.2. Diversity gain

Diversity gain is used in wireless channels to combat fading. The receive antennas see independently faded versions of the same signal. The receiver combines these signals so that the resultant signal presents reduced fading in comparison with the signal at any one antenna, improving the signal-to-noise ratio (SNR) of the received signal. Diversity gain in MIMO systems represents the improvement of SNR, averaged in time, respect to the SNR of the best channel SISO.

2.4.3. Array gain

Is the average increase in the SNR at the receiver that arises from the coherent combining effect of multiple antennas at the receiver or transmitter or both.

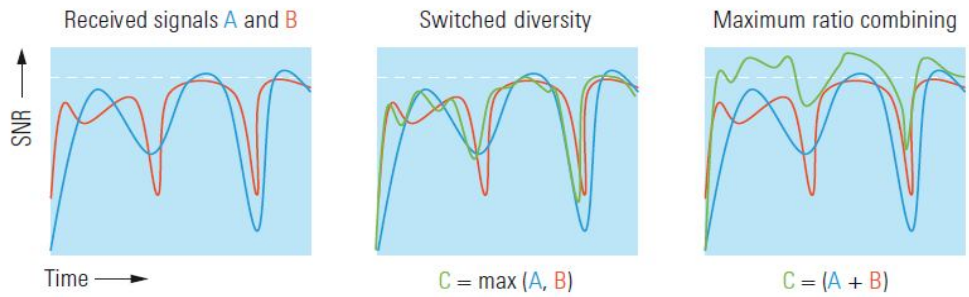

FIGURE 2.2.3. SIGNAL COMBINING

These properties, spatial diversity, spatial multiplexing and array gain, cannot be applied simultaneously.

2.5. Spatial diversity

2.5.1. Spatial Diversity in Reception

The diversity in reception is a widely technique used to reduce the fading due to multipath and improve the SNR. The spatial diversity uses several antennas separated a certain distance, each of the antennas receive a replica of the transmitted signal. If the separation among reception antennas is enough, the fading suffered for each channel will be independent and the signal received won't suffer a simultaneously fading. The most important techniques in spatial diversity in reception are:

- Selection combining
- Maximal ratio combining
- Equal Gain Combining

2.5.2. Spatial Diversity in Transmission

The objective is the same than in spatial diversity in reception, reduce the fading. It is a technique more complex. The transmitted signals are combined spatially before arrive to the receiver, hence it is necessary a transmission and reception processing. If it is not available a feedback channel, the transmitter unknown the channel state and it cannot adapt the transmission strategy to the channel state.

2.5.2.1. Space-time coding

The goal of this coding is to maximize the gain by spatial diversity of MIMO channel through the appropriate space-time code generation. The coding is realized both in space as in time, to introduce correlation among the transmitted signals from several antennas

in different temporal periods. This space-time correlation is used to take advantage of the MIMO channel fading and to minimize the errors introduced by the channel.

This coding improves the link performance achieving spatial diversity in transmission without increasing the wideband.

Different encodings are considered:

- Space-time Trellis codification (STTC)
- Space-time block codification (STBC)

2.5.2.2. Spatial multiplexing

The goal of spatial multiplexing, in contrast to space-time coding, is to maximize the transmission rate, i.e. the spectral efficiency. It transmits independent information fluxes for each antenna, using all of them the same wideband and the same temporal slot. Thanks to the decorrelation among the channels produced by multipath and channel knowledge in the receiver it is possible to separate the different information fluxes. In a MxN system, M independent symbols are transmitted simultaneously in a symbol period.

These are some options of codification with spatial multiplexing:

- Horizontal Coding HE (H-BLAST)
- Vertical Coding VE (V-BLAST)
- HE and VE combination (D-BLAST)

2.6. Spatial correlation

As well as the classic diversity systems, the MIMO systems require that the different subchannels are as independent as possible. The presence of correlation reduces the diversity gain and therefore part of the potential offered by MIMO systems. The correlation impact in equivalent MIMO system is reflected in the gain of the generated equivalent subchannels, i.e. in the magnitude of the eigenvalues. As the correlation increases, the eigenvalues spread is bigger. The correlation is at least one of the limiter factors of the diversity system performance.

The spatial correlation principally is influenced by the richness of the scatterers in the environment but it is also being influenced by other factors like the gap among the array elements or the orientation between arrays, the array topology or even the radiation diagram of the antenna.

The fading suffered by the different generated subchannels between each pair of transmitter and receiver antennas are independent, thanks of that are obtained high spectral efficiencies.

The presence of correlation among subchannels degrades the system performance; hence, the correlation is a key parameter in the use of multiple antennas since it determines the diversity system efficiency.

The correlation is defined for different fields, in space, in time and in frequency; in case of spatial diversity is talked about spatial correlation to indicate the statistical similarity grade between two channels which transmitter and receiver antennas are separated by a certain distance.

2.7. Capacity

The performance measurement of a MIMO channel is studied as well through the bit error probability or through the channel capacity. This represents the highest spectral efficiency and, in contrast to the bit error probability, it allows to evaluate the channel with independence of the transmission and codification scheme used. The channel capacity depends both on the signal-to-noise ratio in the receiver and the eigenvalues of HH^H.

The correlation among the subchannels is one factor that affects the capacity behaviour. The presence of correlation eases the diversity grade and reduces the channel capacity respect to the uncorrelated channel.

The eigenvalues allow evaluating the MIMO channel performance without the complexity that introduces the correlation study and without the dependency between the capacity and the signal-to-noise ratio.

2.8. Analytical channel models

Analytical channel models focus, up to now, on modelling only the spatial structure and provide a mathematical representation of the channel matrix [9][10]. They describe the impulse response of the channel between the elements of the antenna arrays at both link ends by providing analytical expressions for the channel matrix. They are very popular for developing MIMO algorithms in general.

2.8.1. Simplified representations of Gaussian MIMO channels

It is assumed be working with Rayleigh channels if this assumption is not fulfilled, all the following models will inevitably fail.

It is required the characterization of the entire correlation matrix to easily treat it and analyze it because its dimensions rapidly increase as the array sizes increase.

They are considered four correlation-based analytical models:

2.8.1.1. Kronecker model

Simplifies the expression of the full correlation matrix by using a separability assumption

$$R = R_r \otimes R_t \tag{21}$$

where R_t and R_r are the transmit and receive correlation matrices respectively.

$$\begin{aligned} R_t &= \mathcal{E}\{H^H H\}/N_R \\ R_r &= \mathcal{E}\{(HH^H)^T\}/N_T \end{aligned} \tag{22}$$

The Kronecker model is valid when the transmit and receive correlation coefficients are independent of the considered receive and transmit antenna respectively, irrespective of antenna configurations and intra-array spacings [10].

The channel matrix may be expressed as:

$$\widetilde{H} = R_r^{1/2} H_w R_t^{1/2} \tag{23}$$

This model became popular because of its simple analytic treatment. However, the main drawback of this model is that it forces both link ends to be separable, irrespective of whether the channel supports this or not.

2.8.1.2. Eigenbeam model from Weichselberger model

The idea consists in relax the separability restriction of the Kronecker model and to allow for any arbitrary coupling between transmit and receive eigenbase, i.e. to model the correlation properties at the receiver and transmitter jointly. To derive the eigenbeam model of a Rayleigh channel, they are defined the eigenvalue decompositions of receive and transmit correlation matrices:

$$R_r = U_{R_r} \Lambda_{R_r} U_{R_r}^H \tag{24}$$

$$R_t = U_{R_t} \Lambda_{R_t} U_{R_t}^H \tag{25}$$

The channel matrix can be characterized by:

$$\widetilde{H} = U_{R_r}^{*} H_e U_{R_t}^{H} \quad (26)$$

Where H_e is a fading matrix relating receive and transmit eigenmodes. The eigenbeam model is the based on the assumption that all transmit and receive eigenmodes are mutually completely uncorrelated. The channel also can be expressed as:

$$\widetilde{H} = U_{R_r}^{*} (\Omega_e \odot H_w) U_{R_t}^{H} \quad (27)$$

where H_w is an i.i.d complex Gaussian random fading matrix and Ω_e is the power coupling matrix. This model is a good approximation and has a good performance-complexity compromise [9] [10].

2.8.1.3. Virtual channel representation:

It models the MIMO channels in the beamspace instead of the eigenspace. In particular, the eigenvectors are replaced by fixed and predefined steering vectors. The channel matrix can be expressed as:

$$\widetilde{H} = \hat{A}_r H_v \hat{A}_t^{T} \quad (28)$$

The VCR can be easily interpreted. Its angular resolution, and hence 'accuracy', depends on the actual antenna configuration, its accuracy increases with the number of antennas, as angular bins become smaller [9] [10].

Chapter 3.

Process

The goal of this study in MIMO systems is to find if the MIMO system measured in the October 2009 campaign and specified on Part0 can be characterized by the Kronecker model. Hence, we need to obtain the channel matrix and with it obtain the spatial correlation matrix. Then we obtain the Kronecker model correlation matrix and finally we compare it with the spatial correlation matrix. We explain the process in this chapter.

There is a distinction among link mobility types:

- ***Static or nomadic*:** all the nodes of the link, transmitters and receivers, are static.
- ***Single-mobile*:** one node of the link is mobile and the other is static.
- ***Double-mobile*:** all the nodes of the link are mobile.

Also there is a distinction between scenarios explained in Part0. These are the specified scenarios:

- ***8s:*** all 8 nodes are static, with no people in the area.
- ***8sp:*** all 8 nodes are static, with people passing by.
- ***8ms:*** 4 nodes are moving locally over a small range and 4 nodes are static.
- ***8rms:*** 2 nodes are moving along routes in the corridor, 2 nodes are moving locally over a small range and 4 nodes are static.

3.1. Obtaining the Channel Matrix

The result of made the measures specified in Part0 was the channel matrix H with dimensions *t x f x l*, time, frequency and link number respectively. Each link is composed by one transmitter and one receiver and what we have in MIMO systems is an *N x M* system, consisting on the transmission among *N* transmitter and *M* receiver antennas, therefore, we considered that one MIMO channel is composed by various links, concretely, *N x M* links. For that reason, we need to adapt the original *H* to an *H* adequate that contemplates the channels as a composition of *N x M* links. The dimensions of this matrix might be *N x M x t x f x ch*, transmitters, receivers, time, frequency and channel. We work with distributed MIMO channels 2x2. In this system we have 2 transmitters and 2 receivers, if initially we have 64 valid links, this MIMO system will consist in 16 channels as each channel is composed by 4 (2x2) subchannels, links. We have built a table with the relation between each link and its

corresponding channel that simplifies the conversion matrix process. Finally our channel matrix has this form:

$$H(:,:,t,f,ch) = \begin{pmatrix} h_{11}(t) & h_{12}(t) & \cdots & h_{1M}(t) \\ h_{21}(t) & h_{22}(t) & \cdots & h_{2M}(t) \\ \vdots & \vdots & \ddots & \vdots \\ h_{N1}(t) & h_{N2}(t) & \cdots & h_{NM}(t) \end{pmatrix} \quad (29)$$

3.2. Obtaining the Spatial Correlation Matrix

Before obtaining the spatial correlation matrix *R* we have to normalize the channel matrix, that means remove the path loss, the static shadowing and the dynamic shadowing, that way we just have the fading. To normalize the channel we have to obtain the average power for each channel, obtaining first the *Ps* for each link like we did in SISO fading but without frequency subbands:

$$Ps(n,m,f,t,ch) = \frac{1}{T_{av}} \sum_{t'=t-\frac{T_{av}}{2}}^{t+\frac{T_{av}}{2}-1} |H[n,m,t',f,ch]|^2 \quad (30)$$

And then the average power for each channel is:

$$P_{channel}(t,f,ch) = \sum_{n=1}^{N} \sum_{m=1}^{M} Ps(n,m,t,f,ch) \Big/ NM \quad (31)$$

Finally the normalized channel matrix *G* is obtained by:

$$G(n,m,t,f,ch) = \frac{H(n,m,t,f,ch)}{\sqrt[2]{P_{channel}(t,f,ch)}} \quad (32)$$

Once we have the channel matrix normalized we obtain the spatial correlation channel matrix *R* as:

$$R = \mathcal{E}\{vec(H^H)vec(H^H)^H\} \quad (33)$$

The matrix is an *NM x NM* positive semi-definite Hermitian matrix, which describes the correlation between all pairs of transmit-receive channels.

We define and obtain too the transmit and receive correlation matrices R_t and R_r as (22).

These we will be used to obtain the Kronecker correlation matrix.

For the R, R_t and R_r matrices we make the average in frequency and with the time grouping it in time bins to realize the expectation factor and study the correlation in time bins.

3.3 Obtaining the Kronecker Model Correlation Matrix

The Kronecker model correlation matrix as we explained in chapter 2 is obtained by the Kronecker product between transmit and receive correlation matrices (21).

3.4. Comparing Models and Correlation Matrices

The correlation matrix R is highly representative of the spatial richness of the channel; hence, we can compare models or models with measured channels by comparing their correlation matrices.

We consider two ways to compare an approximated correlation matrix R' and the channel correlation matrix R, one is given by the difference or the error between them:

$$\Psi = \frac{\|R - R'\|_F}{\|R\|_F} \tag{34}$$

And the other one is given by the distance between both correlations:

$$d_{corr} = 1 - \frac{Tr\{RR'\}}{\|R\|_F \|R'\|_F} \tag{35}$$

If the distance is equal to zero the correlation matrices are identical and if it is equal to one, they differ in the largest possible way. [10]

Chapter 4.

Results

In this chapter we present the results of comparing the space correlation matrix *R* and the Kronecker model correlation matrix *R'*. We also show the results of derivate studies from that comparison. For almost all the studies we contemplate the different scenarios and mobility types mentioned in the previous chapter.

The spatial correlation matrix *R* is not normalized, hence, the values of the correlation coefficients are higher than 1 conserving the major values in the diagonal as they are the autocorrelation coefficients.

4.1. Evolution of Ψ and d_{corr} in time

The following graphs represent the evolution of Ψ and d_{corr} in time for each type of mobility. In these graphs are grouped all the channels from the different scenarios considering the mobility type.

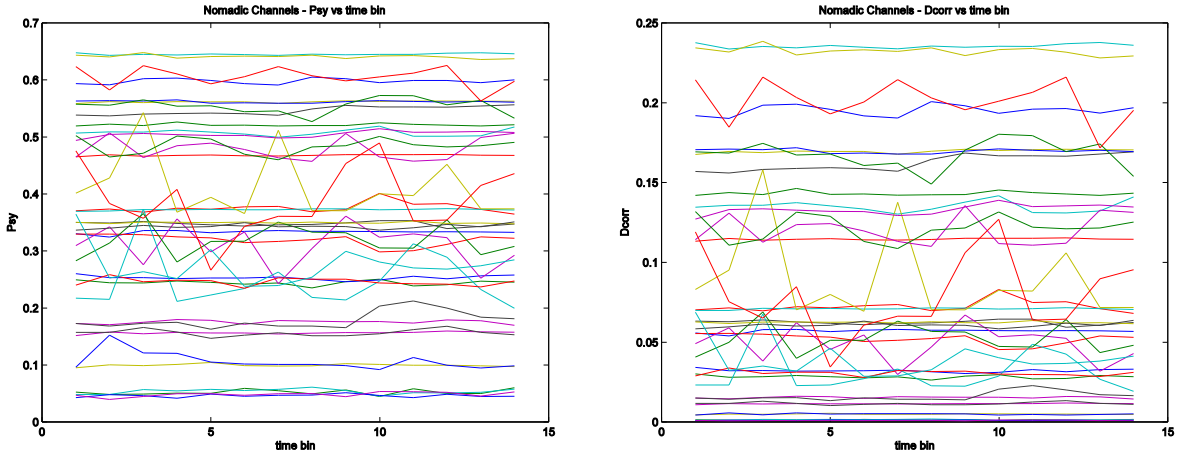

FIGURE 2.4.1. EVOLUTION OF Ψ AND D_{CORR} IN TIME - STATIC LINKS

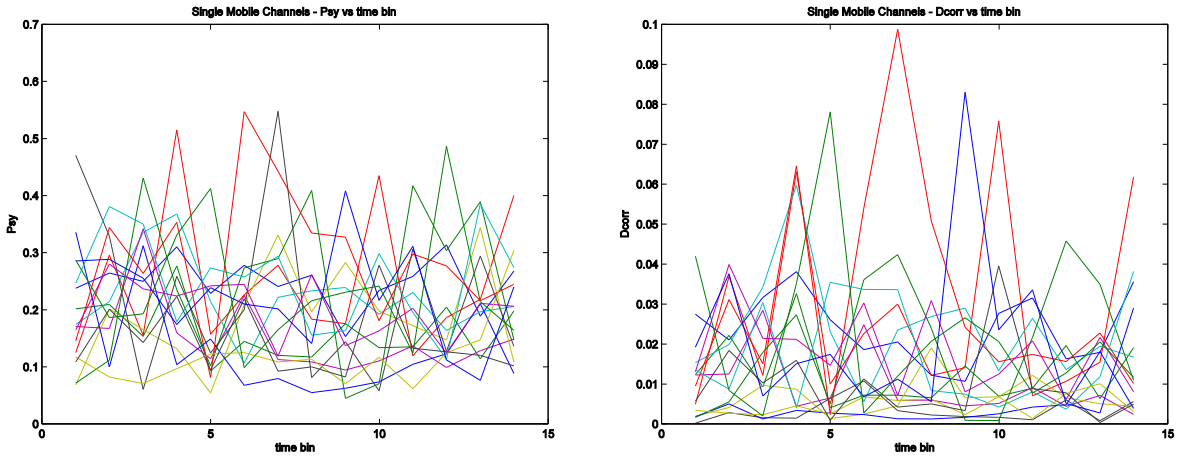

FIGURE 2.4.2. EVOLUTION OF Ψ AND D_{CORR} IN TIME - SINGLE-MOBILE LINKS

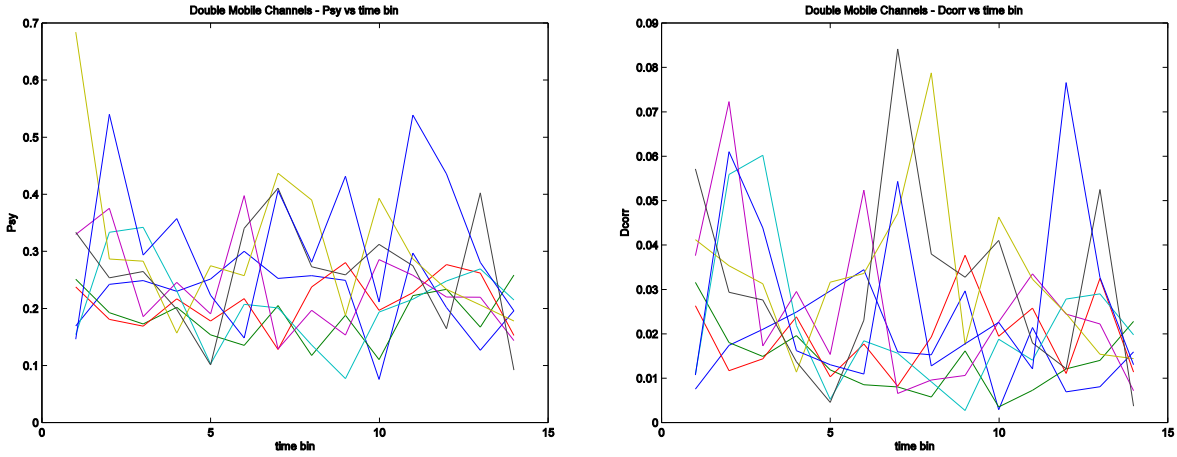

FIGURE 2.4.3. EVOLUTION OF Ψ AND D_{CORR} IN TIME - DOUBLE-MOBILE LINKS

In general the values of d_{corr} in all the mobility types are relatively lower, 0.24 is the maximum for static links. These values are lower in mobile nodes. In static links the values are practically constant over the time, except for some channels of the 8sp scenario. For mobile links the values are variable over the time but these variations are small.

With this we can say that the difference between the correlation matrix *R* and the Kronecker model correlation matrix *R'* is small for all the scenarios and all types of mobility and does not vary too much over the time.

The following tables show the error Ψ and difference d_{corr} between the Kronecker model correlation matrix and spatial correlation matrix for all the scenarios in all the time bins divided in mobility types (Static as S, Single-Mobile as SM and Double-Mobile as DM). These values are an average over all the subchannels.

Scn	Mobity	Time bin													
8s	S	0,358	0,357	0,359	0,360	0,359	0,358	0,358	0,359	0,360	0,362	0,361	0,360	0,360	0,360
8sp	S	0,351	0,361	0,377	0,354	0,351	0,351	0,360	0,349	0,356	0,355	0,361	0,365	0,346	0,349
8ms	S	0,306	0,310	0,312	0,309	0,311	0,312	0,309	0,310	0,313	0,312	0,311	0,313	0,311	0,313
	SM	0,223	0,223	0,222	0,266	0,142	0,182	0,242	0,155	0,166	0,179	0,183	0,171	0,212	0,194
	DM	0,203	0,237	0,233	0,220	0,172	0,215	0,197	0,187	0,199	0,144	0,241	0,240	0,206	0,206
8rms	S	0,347	0,285	0,284	0,303	0,279	0,274	0,277	0,287	0,320	0,331	0,291	0,289	0,305	0,316
	SM	0,178	0,234	0,243	0,227	0,196	0,247	0,214	0,216	0,183	0,196	0,218	0,208	0,220	0,210
	DM	0,373	0,364	0,257	0,240	0,197	0,286	0,346	0,285	0,258	0,301	0,340	0,264	0,277	0,152

TABLE 2.4.1. ψ(R, R') FOR 2X2 SYSTEM

Scn	Mobity	Time bin													
8s	S	0,085	0,085	0,086	0,086	0,086	0,085	0,085	0,086	0,087	0,087	0,087	0,087	0,086	0,086
8sp	S	0,084	0,086	0,094	0,084	0,083	0,083	0,087	0,082	0,086	0,085	0,086	0,088	0,081	0,082
8ms	S	0,062	0,064	0,065	0,064	0,064	0,065	0,063	0,064	0,065	0,065	0,065	0,065	0,065	0,065
	SM	0,010	0,016	0,016	0,026	0,010	0,012	0,012	0,011	0,010	0,017	0,013	0,010	0,011	0,019
	DM	0,019	0,026	0,028	0,023	0,014	0,020	0,012	0,012	0,022	0,011	0,017	0,014	0,021	0,017
8rms	S	0,080	0,055	0,054	0,062	0,053	0,051	0,051	0,055	0,069	0,075	0,056	0,056	0,063	0,066
	SM	0,013	0,019	0,013	0,023	0,020	0,023	0,027	0,019	0,019	0,015	0,015	0,013	0,016	0,014
	DM	0,037	0,050	0,030	0,018	0,016	0,030	0,048	0,035	0,020	0,033	0,024	0,034	0,031	0,010

TABLE 2.4.2. D_{CORR}(R, R') FOR 2X2 SYSTEM

The values of the correlation distance d_{corr} are practically 0 for all the scenarios and all types of mobility over time. We consider that the Kronecker model models well our MIMO channel system.

4.2. Relation between d_{corr} and α

The following figures represent the relation between d_{corr} and alpha, which is the Double Rayleigh component result of the SOSF distribution fitting as it is explained on Part1-Chapter2 related to the fading.

For nomadic channels the fading is supposed to be Ricean, for that reason we do not consider it for this study. We just contemplate the relation between these two parameters for Single Mobile and Double Mobile channels.

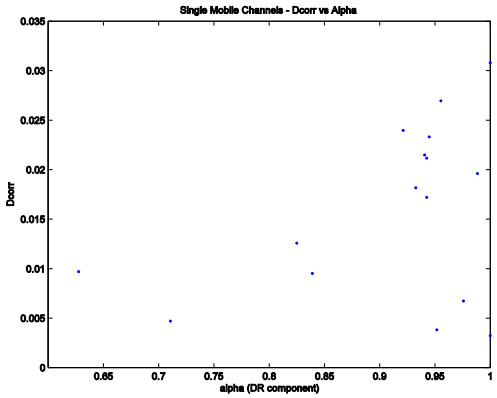

FIGURE 2.4.5. D_{CORR} VS α FOR SINGLE-MOBILE LINKS

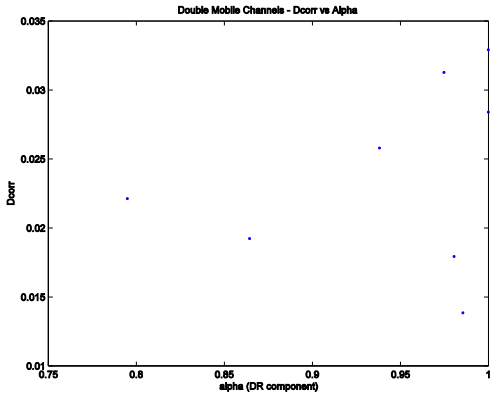

FIGURE 2.4.6. D_{CORR} VS α FOR DOUBLE-MOBILE LINKS

It is observed that the alpha values are high, near 1, this means that the fading for both mobility types is characterized by a Double Rayleigh distribution as we observed in the single antenna analysis. Even though there are not a lot of points to fit well a relation between d_{corr} and alpha, we can observe a trend toward the increase of the distance correlation as alpha increases.

4.3. Relation between d_{corr} and Distance among nodes

Here we analyze if there is a relation between the distance among nodes and the distance between the correlation matrices *R* and *R'*.

Observing the following figures we can conclude that there is no relation between these parameters.

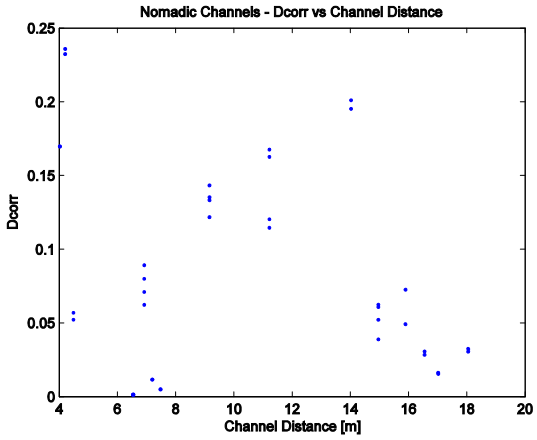

FIGURE 2.4.7. D_{corr} VS DISTANCE FOR NOMADIC LINKS

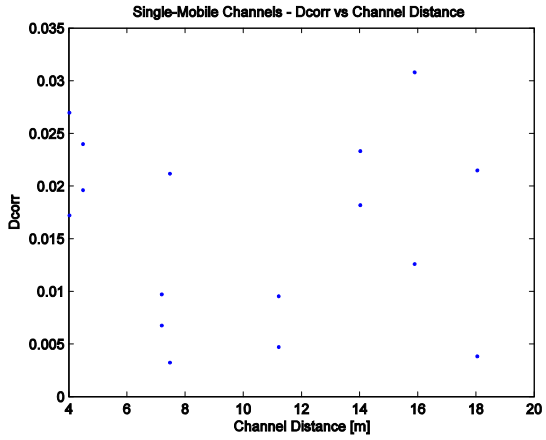

FIGURE 2.4.8. D_{corr} VS DISTANCE FOR SINGLE-MOBILE LINKS

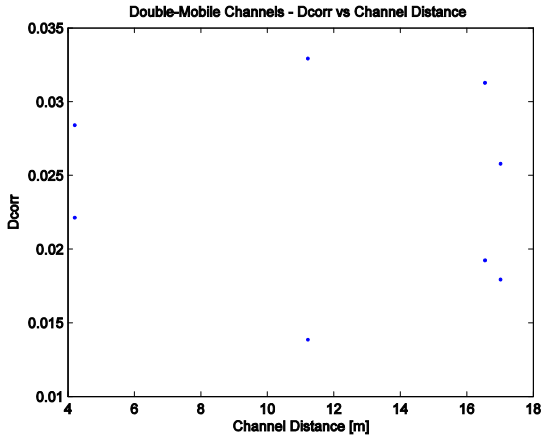

FIGURE 2.4.9. D_{corr} VS DISTANCE FOR DOUBLE-MOBILE LINKS

Chapter 5.

Conclusions

This part has presented an analysis and modelling of indoor-to-indoor MIMO channels based on experimental results. Concretely, this study has focused on checking whether measured MIMO channel can be modelled with the Kronecker model. There are the main conclusions:

- The analysis is based on a wideband experimental campaign at 3.8 GHz.
- We separate the static, single mobile and double mobile nodes to find if there are different behaviours for the elements studied.
- We obtain the spatial correlation matrix R from the channel matrix, obtained in turn from the channel measurements.
- We obtain the Kronecker correlation matrix R' from transmit and receive correlation matrices.
- The distance correlation between R and R' is practically 0 for all scenarios and all mobility types. The Kronecker model can model the MIMO channels measured.
- Like in single antenna analysis, for both double-mobile and single-mobile nodes, fading behaviour is characterized by Double-Rayleigh distribution.
- We think that there is a relation between the increase of the distance correlation as alpha increases.
- There is no relation between the distance correlation and the channel distance.

BIBLIOGRAPHY

[1] *"PUCCO Radio Measurement Campaign"*, October 2009.

[2] S. Saunders, *Antennas and Propagation for Wireless Communication Systems*, Wiley, 2000

[3] J. D. Parsons, *The Mobile Radio Propagation Channel*, Pentech Press, 1992

[4] C. Oestges, N. Czink, B. Bandemer, P. Castiglione, F. Kaltenberger and A. Paulraj, *Experimental Characterization and Modeling of Outdoor-to-Indoor and Indoor-to-Indoor Distributed Channels*, December 2009

[5] Fabio Belloni. *Fading Models*, Autumn 2004.

[6] Robert Wilson, *Propagation Losses Through Common Building Materials*, August 2002

[7] John C. Stein, *Indoor Radio WLAN Performance. Part II: Range Performance in a Dense Office Environment*

[8] Jonas Medbo, Jan-Erik Berg, *Simple and Acurate Path Loss Modeling at 5GHz in Indoor Environments with Corridors*,2000

[9] Hüseyin Özcelik, Nicolai Czink, Ernst Bonek. *What makes a Good MIMO Channel Model?*

[10] C. Oestges, B. Clerckx. *MIMO Wireless Communications – From Real-World Propagation to Space-Time Code Design*, Ed. Academic Press, 2007

[11] A. Paulraj, R. Nabar and D. Gore. *Introduction to Space-Time Wireless Communications*, Ed. Cambridge University Press, 2003

[12] O. Fernandez. *Caracterización Experimental y Modelado de Canal MIMO para aplicaciones WLAN y WMAN*, 2007